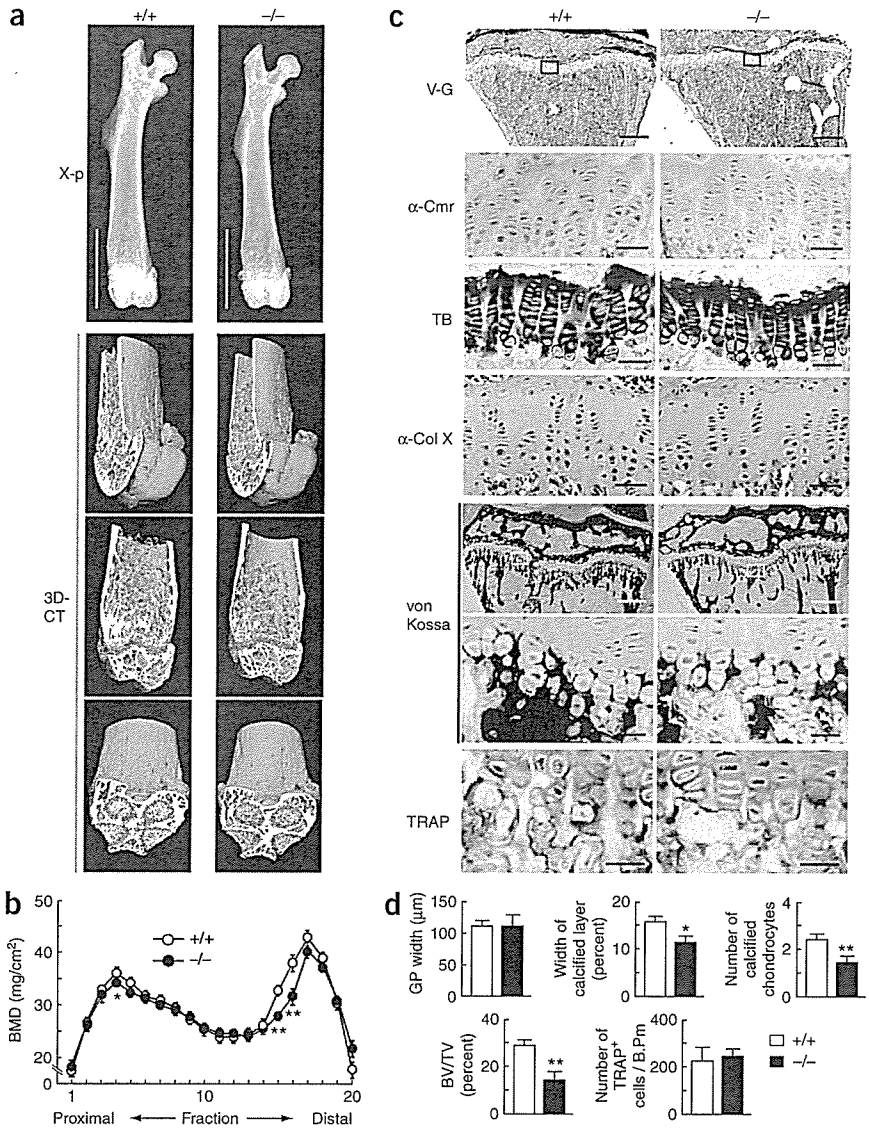

Figure 2 Radiological and histological findings of the long bones in wild-type (*Cst10*$^{+/+}$) and *Cst10*$^{-/-}$ littermates at 8 weeks of age under physiological conditions. (**a**) Plain X-ray of whole femurs, and three-dimensional computed tomography images of the distal part shown as green lines on the plain X-ray. (**b**) Bone mineral density (BMD) of the 20 equally divided fractions of femurs. (**c**) Histological findings of the proximal tibias. Villanueva-Goldner staining (V-G; scale bar, 200 μm). Inset boxes indicate the regions of the following three rows: immunostaining with an antibody to carminerin (α-Cmr; scale bar, 20 μm), toluidine blue staining (TB; scale bar, 20 μm), immunostaining with an antibody to Col X (α-Col X; scale bar, 20 μm). von Kossa staining (scale bars, 200 μm (top) and 20 μm (bottom)). Inset boxes indicate the regions of the bottom two rows: von Kossa staining and TRAP staining (scale bar, 20 μm). (**d**) Histomorphometric analyses of the growth plate and primary spongiosa just beneath it. The entire growth plate width (GP width) was measured on the TB sections, and the percent width of calcified layer to the entire growth plate and the number of calcified chondrocytes per column were measured on the von Kossa sections. Bone volume/tissue volume (BV/TV) and the number of TRAP$^+$ cells in 100 mm of bone perimeter were measured in the primary spongiosa. Data are expressed as mean ± s.e.m. for 15 mice per group. $^*P < 0.05$, $^{**}P < 0.01$ compared to wild-type mice.

control the level of PPi in the cultured growth-plate chondrocytes, including: NPP1, which generates PPi from nucleoside triphosphates using nucleoside triphosphate pyrophosphohydrolase (NTPPPH) activity[8], tissue-nonspecific alkaline phosphatase (TNAP) which hydrolyzes PPi[9], and the multiple-pass transmembrane protein ANK, which mediates intracellular-to-extracellular channeling of PPi[10]. Among these proteins, the carminerin deficiency upregulated expression of only NPP1, and accordingly, increased NTPPPH activity (**Supplementary Fig. 3**). The reintroduction of carminerin into *Cst10*$^{-/-}$ chondrocytes (Ax-*Cmr*) restored the abnormalities in calcification, expression of NPP1 and NTPPPH activity to those similar to the wild-type culture (**Supplementary Fig. 3**). The promoter activity of an *Enpp1* promoter-luciferase construct (–964 *Enpp1* promoter-Luc) transfected into ATDC5 cells overexpressing carminerin (pCMV-*Cmr*/ATDC5) was lower than cells transfected with mock vector (pCMV/ATDC5; **Supplementary Fig. 3**). Deletion analysis of the *Enpp1* promoter region identified the core responsive element between the –360 and –324 regions, within which an SRY (sex-determining region Y) consensus sequence was predicted. Site-directed mutagenesis to eliminate the SRY site canceled the inhibition of *Enpp1* transcription by carminerin. Electrophoretic mobility shift assay confirmed specific binding of the SRY region by an oligonucleotide probe with nuclear extracts prepared from pCMV/ATDC5 and pCMV-*Cmr*/ATDC5 cells. Binding by the probe was weaker with the pCMV-*Cmr*/ATDC5 extracts than with the pCMV/ATDC5 extracts (**Supplementary Fig. 3**). As the binding was not detected using the synthetic carminerin protein instead of the nuclear extracts, carminerin itself was shown not to be the direct transcription factor for the SRY region. In contrast, nuclear extracts from the primary *Cst10*$^{-/-}$ growth plate chondrocytes showed stronger binding with the SRY site than those from the wild-type chondrocytes (**Supplementary Fig. 3**). Hence, the transcriptional inhibition of NPP1 expression by carminerin may result, at least partly, from the impaired binding of a transcription factor to the SRY site of the *Enpp1* promoter. Although Sox9, a potent regulator of chondrocyte differentiation[11,12], is the most probable transcription factor for this site, we did not observe a supershift of the DNA-protein complex when we added Sox9-specific antibody in the electrophoretic mobility shift assay (data not shown), indicating the involvement of other transcription factors in the regulation of the SRY site. In addition, in our efforts to identify the upstream regulator of NPP1, we did not find substantial regulation of expression or transcription of NPP1 by carminerin through the cytokines interleukin-1β (IL-1β), fibroblast growth factor-2 (FGF-2) or transforming growth factor-β (TGF-β), which previously have been reported to regulate NPP1 expression[13–15] (**Supplementary Fig. 4** online). Thus, further studies to elucidate a more detailed mechanism through which carminerin inhibits transcription of NPP1 will be necessary.

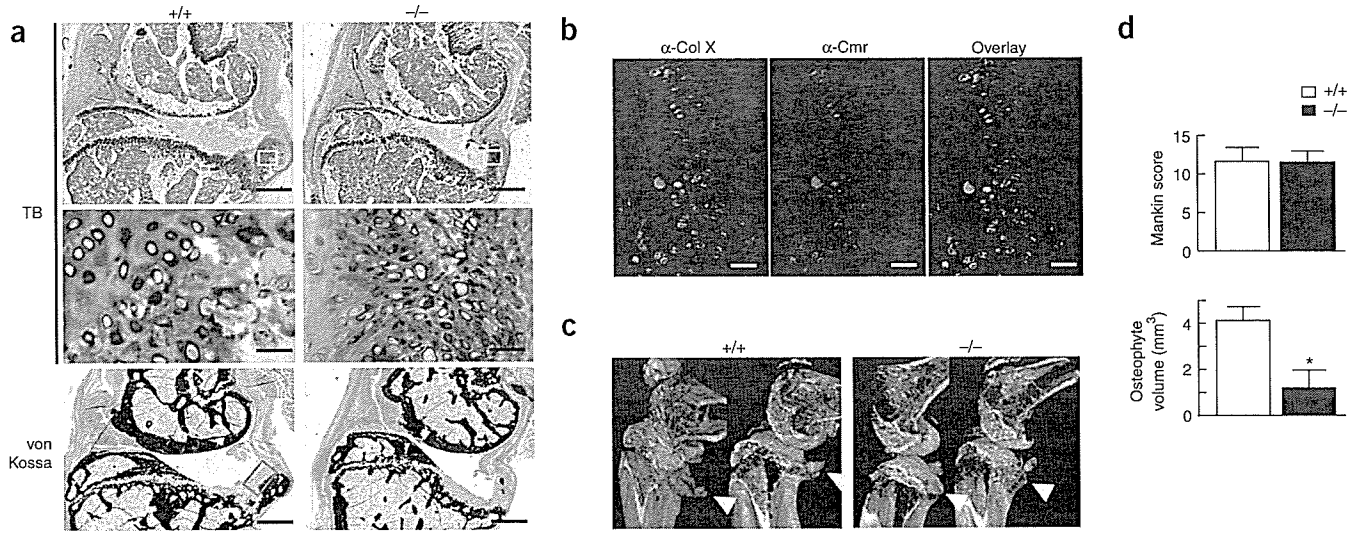

Figure 3 Histological and radiological findings of osteoarthritic joints in wild-type (*Cst10*$^{+/+}$) and *Cst10*$^{-/-}$ littermates. (**a**) Osteoarthritis was induced at the posterior tibias of the knee joint of 8-week-old mice by surgically imposing instability to the joint. Histological features; toluidine blue (TB; inset boxes in the top figures indicate regions shown in middle row; scale bars, 200 μm (top) and 20 μm (middle)) and von Kossa stainings (scale bar, 200 μm) of the sagittal sections of knee joints 10 weeks after surgery (left side of each photo is anterior side). (**b**) Immunostainings with an antibody to Col X (α-Col X, green), an antibody to carminerin (α-Cmr, red) and the overlay (yellow) analyzed by confocal microscopy in the region indicated in the inset of the image of von Kossa staining of wild-type knee in **a**. Scale bar, 20 μm. (**c**) Three-dimensional computed tomography images of the knee joints from the posterolateral projection. Arrowheads indicate osteophytes. (**d**) Quantification of the cartilage destruction and the osteophyte formation as determined by the Mankin grading score (top) and the osteophyte volume measured on the three-dimensional computed tomography images (bottom), respectively. Data are expressed as mean ± s.e.m. for ten mice per group. $^{*}P < 0.01$ compared to wild-type mice.

Finally, we carried out *in vitro* fertilization and embryo transfer from *Cst10*$^{-/-}$ mice and the *Enpp1*$^{-/-}$ mice, which lack expression of functional NPP1 (ref. 16), and generated four genotypes of mice: *Cst10*$^{+/+}$*Enpp1*$^{+/+}$, *Cst10*$^{-/-}$*Enpp1*$^{+/+}$, *Cst10*$^{+/+}$*Enpp1*$^{-/-}$ and *Cst10*$^{-/-}$*Enpp1*$^{-/-}$. When we used the experimental models, there was no difference in formation of osteoarthritic osteophytes, age-related ectopic ossification or high phosphate–induced auricular ossification between the NPP1-deficient mice (*Cst10*$^{+/+}$*Enpp1*$^{-/-}$) and the double-deficient mice (*Cst10*$^{-/-}$*Enpp1*$^{-/-}$), confirming that functional NPP1 is essential for suppression of the pathological endochondral ossification by the carminerin deficiency *in vivo* (**Supplementary Fig. 5** online).

Our previous *in vitro* study showed that overexpression of carminerin in ATDC5 cells accelerated not only calcification but also

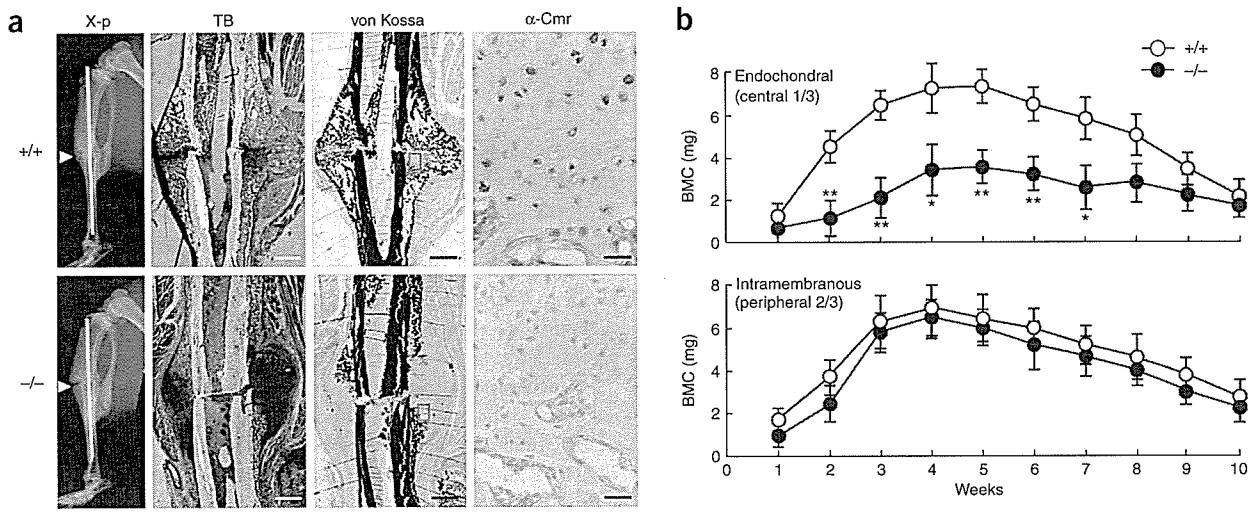

Figure 4 Radiological and histological findings of bone fracture healing in wild-type (*Cst10*$^{+/+}$) and *Cst10*$^{-/-}$ littermates. Fracture was produced by a transverse osteotomy that was stabilized with an intramedullary nail at the midshaft of tibias in 8-week-old mice. (**a**) Plain X-ray, toluidine blue (TB), von Kossa and a carminerin-specific antibody (α-Cmr) immunostainings 3 weeks after fracture. Insets in the image of von Kossa staining indicate regions of immunostaining. Scale bar, 20 μm for immunostaining, and 200 μm for the others. (**b**) Time course of bone mineral content (BMC) at the fracture callus for 10 weeks after fracture. BMC of the central one-third portion was measured as the endochondral ossification, and BMC of the peripheral two-thirds as the intramembranous ossification. Data are expressed as mean ± s.e.m. for six mice per time per group. $^{*}P < 0.05$, $^{**}P < 0.01$ compared to wild-type mice.

hypertrophic differentiation[1]. In contrast, the present *in vivo* and *in vitro* studies on deficiency of carminerin showed no abnormality in hypertrophic differentiation of chondrocytes. This discrepancy might owe to the involvement of insulin signaling by way of NPP1 regulation because in addition to the enzymatic function of synthesizing PPi, NPP1 is known to suppress the tyrosine kinase activity of the insulin receptor[17]. Considering that our previous ADTC5 cell culture was carried out in the presence of insulin (10 μg/ml), which was essential to induce hypertrophic differentiation[18], overexpression of carminerin might cause suppression of NPP1, which in turn increases sensitivity to insulin and enhances hypertrophic differentiation. The fact that the serum insulin levels in wild-type and *Cst10*$^{-/-}$ mice were similar (0.32 ± 0.08 and 0.35 ± 0.06 ng/ml, respectively; mean ± s.e.m. of five mice per genotype) and were much lower than the *in vitro* concentration, indicates that the regulation of chondrocyte calcification by endogenous carminerin *in vivo* was not mediated by insulin signaling.

Pi has been suggested to be rate limiting for calcification, which may explain why clinical disorders in homeostasis of Pi lead to, for example, rickets, osteomalacia[19] and ectopic calcification[20]. Considering that carminerin was isolated as a protein that was upregulated by a high-phosphate diet in association with calcification of mouse auricular cartilage, carminerin might partly mediate Pi-induced cartilage calcification. In fact, carminerin deficiency decreased calcification of auricular cartilage in wild-type mice on a high-phosphate diet (**Supplementary Fig. 5**). Carminerin may therefore be the first cartilage-specific protein that induces chondrocyte calcification during endochondral ossification under physiological and pathological conditions.

METHODS

Generation of *Cst10*$^{-/-}$ mice. We obtained a *Cst10* genomic clone by screening a bacterial artificial chromosome (BAC) library using a BAC PCR screening system (Genome Systems). We used a 120-kb fragment of a BAC clone containing all exons (1–3) of *Cst10* to construct the targeting vector. We constructed the targeting vector to replace exon 1, including the transcription initiation site, by the neomycin-resistance gene. We introduced the linearized targeting vector by electroporation into embryonic stem (ES) cells as previously described[21], and identified two independent targeted ES cell clones by Southern blot analysis, using 5′ (probe 1) and 3′ (probe 2) external probes. We generated chimeric males and crossed them with C57BL/6 females, and verified germline transmission by Southern blot analysis. All *Cst10*$^{-/-}$ mice used in this study had been backcrossed for ten generations into the C57BL/6 background. We used RT-PCR to determine the presence of the *Cst10* transcripts. We determined presence of carminerin protein by western blot analysis, as previously described, using a polyclonal antibody to the full-length carminerin protein, which was raised in rabbits using a synthetic peptide of carminerin[1].

Mice conditions. We fed mice a standard rodent diet (CE-2; CLEA Japan) or a high-phosphate diet containing 1.86% phosphorus. In each experiment, we compared littermate wild-type and *Cst10*$^{-/-}$ mice generated from the intercross between heterozygous mice. All experiments were performed on male mice, according to the protocol approved by the Animal Care and Use Committee of the University of Tokyo.

Skeletal preparations. We fixed whole skeletons of wild-type and *Cst10*$^{-/-}$ littermate embryos (E17.5) in 99.5% ethanol, transferred them into acetone and stained them as previously described[21]. We kept specimens in 20% glycerol-1% KOH until skeletons became clearly visible.

Radiological analyses. We took plain radiographs using a soft X-ray apparatus. We measured the bone mineral density (BMD) of the 20 equally divided fractions of the entire femur and bone mineral content (BMC) of the fracture callus with dual energy X-ray absorptiometry using a bone mineral analyzer. We carried out micro–computed tomography scanning using a composite X-ray analyzer, and reconstructed cross-sectional tomograms of 10 μm thickness at 12 × 12 pixels into a three-dimensional feature by the volume-rending method; we then measured the ossification volume using a computer. We performed peripheral quantitative computed tomography scans at the metaphysis of 0.2 mm below the proximal growth plate and at the midshaft of tibias.

Histological analyses. For Villanueva-Goldner, toluidine blue and von Kossa stainings, we fixed samples with 70% ethanol, embedded them in glycol methacrylate without decalcification and sectioned them into 3-μm slices. We carried out histomorphometric analyses in the growth plate, primary spongiosa just beneath it (0.3 mm in length) and secondary spongiosa (1.0 mm in length from 0.3 mm below the growth plate) of the proximal tibias and the fifth vertebra using an image analyzer. For double labeling to analyze the dynamic bone remodeling, we subcutaneously injected mice with 8 mg/kg body weight of calcein at 10 d and 3 d before killing. We stained TRAP^{+} cells at pH 5.0 in the presence of L(+)-tartaric acid using naphthol AS-MX phosphate in *N,N*-dimethyl formamide as the substrate. We performed histomorphometric measurements in eight optical fields, according to the American Society for Bone and Mineral Research nomenclature report[22], and calculated the averages per mouse. For H&E staining, we perfused mice with 4% buffered paraformaldehyde, decalcified bones with 4.13% EDTA, embedded them in paraffin, and cut them into 6 μm–thick sections. For immunohistochemical analyses, we treated sections as previously described[4], using polyclonal rabbit antibody to carminerin or Col X (Santa Cruz Biotechnology). For double staining, we treated sections with 1% BSA, incubated them with a mixture of carminerin-specific antibody and mouse monoclonal Col X–specific antibody and with Texas red-conjugated goat antibody to rabbit IgG. They were then reacted with biotin-conjugated antibodies to mouse IgG+IgA+IgM and FITC-streptoavidin. The localizations were observed by confocal laser scanning microscopy.

Osteoarthritis model. Eight-week-old mice underwent a microsurgery to produce instability in the knee joints as we reported previously[2]. Mice were killed 10 weeks after surgery, and cartilage destruction was quantified as the Mankin grading score[3] of the most severe change among multiple serial toluidine blue sections in each mouse. We measured osteophyte volume with three-dimensional computed tomography as described above.

Fracture model. We produced fracture at the midshaft of tibias of 8-week-old mice as we reported previously[4,5]. Several mice were killed each week for 10 weeks after the surgery. After the entire callus was longitudinally divided into three equal portions on a bone mineral analyzer image, we measured BMC at the central one-third portion as the endochondral ossification and that at the peripheral two-thirds as the intramembranous ossification. We performed histological analyses 3 weeks after fracture.

Statistical analysis. All data are expressed as mean ± s.e.m. Means of groups were compared by ANOVA and significance of differences was determined by *post hoc* testing using the Bonferroni method.

Note: Supplementary information is available on the Nature Medicine website.

ACKNOWLEDGMENTS

This study was supported by a Grant-in-aid for Scientific Research from the Japanese Ministry of Education, Culture, Sports, Science, and Technology (#14370454), and by the Investigation Committee on the Ossification of Spinal Ligaments, Japanese Ministry of Public Health and Welfare.

COMPETING INTERESTS STATEMENT

The authors declare that they have no competing financial interests.

Published online at http://www.nature.com/naturemedicine/
Reprints and permissions information is available online at http://npg.nature.com/reprintsandpermissions/

1. Koshizuka, Y. *et al.* Cystatin 10, a novel chondrocyte-specific protein, may promote the last steps of the chondrocyte differentiation pathway. *J. Biol. Chem.* **278**, 48259–48266 (2003).
2. Kamekura, S. *et al.* Osteoarthritis development in novel experimental mouse models induced by knee joint instability. *Osteoarthritis Cartilage* **13**, 632–641 (2005).

3. Mankin, H.J., Johnson, M.E. & Lippiello, L. Biochemical and metabolic abnormalities in articular cartilage from osteoarthritic human hips. III. Distribution and metabolism of amino sugar-containing macromolecules. *J. Bone Joint Surg. Am.* **63**, 131–139 (1981).
4. Shimoaka, T. *et al.* Impairment of bone healing by insulin receptor substrate-1 deficiency. *J. Biol. Chem.* **279**, 15314–15322 (2004).
5. Chikuda, H. *et al.* Cyclic GMP-dependent protein kinase II is a molecular switch from proliferation to hypertrophic differentiation of chondrocytes. *Genes Dev.* **18**, 2418–2429 (2004).
6. Wolbach, S.B. Vitamin-A deficiency and excess in relation to skeletal growth. *J. Bone Joint Surg.* **29**, 171–192 (1947).
7. Terkeltaub, R.A. Inorganic pyrophosphate generation and disposition in pathophysiology. *Am. J. Physiol. Cell Physiol.* **281**, C1–C11 (2001).
8. Bollen, M., Gijsbers, R., Ceulemans, H., Stalmans, W. & Stefan, C. Nucleotide pyrophosphatases/phosphodiesterases on the move. *Crit. Rev. Biochem. Mol. Biol.* **35**, 393–432 (2000).
9. Balcerzak, M. *et al.* The roles of annexins and alkaline phosphatase in mineralization process. *Acta Biochim. Pol.* **50**, 1019–1038 (2003).
10. Ryan, L.M. The ank gene story. *Arthritis Res.* **3**, 77–79 (2001).
11. de Crombrugghe, B., Lefebvre, V. & Nakashima, K. Regulatory mechanisms in the pathways of cartilage and bone formation. *Curr. Opin. Cell Biol.* **13**, 721–727 (2001).
12. Akiyama, H., Chaboissier, M.C., Martin, J.F., Schedl, A. & de Crombrugghe, B. The transcription factor Sox9 has essential roles in successive steps of the chondrocyte differentiation pathway and is required for expression of Sox5 and Sox6. *Genes Dev.* **16**, 2813–2828 (2002).
13. Lotz, M. *et al.* Interleukin 1 beta suppresses transforming growth factor-induced inorganic pyrophosphate (PPi) production and expression of the PPi-generating enzyme PC-1 in human chondrocytes. *Proc. Natl. Acad. Sci. USA* **92**, 10364–10368 (1995).
14. Solan, J.L., Deftos, L.J., Goding, J.W. & Terkeltaub, R.A. Expression of the nucleoside triphosphate pyrophosphohydrolase PC-1 is induced by basic fibroblast growth factor (bFGF) and modulated by activation of the protein kinase A and C pathways in osteoblast-like osteosarcoma cells. *J. Bone Miner. Res.* **11**, 183–192 (1996).
15. Oyajobi, B.O., Caswell, A.M. & Russell, R.G. Transforming growth factor beta increases ecto-nucleoside triphosphate pyrophosphatase activity of human bone-derived cells. *J. Bone Miner. Res.* **9**, 99–109 (1994).
16. Okawa, A. *et al.* Mutation in Npps in a mouse model of ossification of the posterior longitudinal ligament of the spine. *Nat. Genet.* **19**, 271–273 (1998).
17. Goldfine, I.D., Maddux, B.A., Youngren, J.F., Trischitta, V. & Frittitta, L. Role of PC-1 in the etiology of insulin resistance. *Ann. NY Acad. Sci.* **892**, 204–222 (1999).
18. Shukunami, C. *et al.* Chondrogenic differentiation of clonal mouse embryonic cell line ATDC5 *in vitro*: differentiation-dependent gene expression of parathyroid hormone (PTH)/PTH-related peptide receptor. *J. Cell Biol.* **133**, 457–468 (1996).
19. Laroche, M. Phosphate, the renal tubule, and the musculoskeletal system. *Joint Bone Spine* **68**, 211–215 (2001).
20. Jono, S. *et al.* Phosphate regulation of vascular smooth muscle cell calcification. *Circ. Res.* **87**, E10–E17 (2000).
21. Nakamichi, Y. *et al.* Chondromodulin I is a bone remodeling factor. *Mol. Cell. Biol.* **23**, 636–644 (2003).
22. Parfitt, A.M. *et al.* Bone histomorphometry: standardization of nomenclature, symbols, and units. Report of the ASBMR Histomorphometry Nomenclature Committee. *J. Bone Miner. Res.* **2**, 595–610 (1987).

Journal of Cellular Biochemistry 99:196–208 (2006)

Regulation of Bone Formation by Adiponectin Through Autocrine/Paracrine and Endocrine Pathways

Yusuke Shinoda,[1] Masayuki Yamaguchi,[1] Naoshi Ogata,[1] Toru Akune,[1] Naoto Kubota,[2] Toshimasa Yamauchi,[2] Yasuo Terauchi,[2] Takashi Kadowaki,[2] Yasuhiro Takeuchi,[3] Seiji Fukumoto,[3] Toshiyuki Ikeda,[1] Kazuto Hoshi,[1] Ung-il Chung,[1] Kozo Nakamura,[1] and Hiroshi Kawaguchi[1]*

[1]Department of Sensory & Motor System Medicine, Faculty of Medicine, University of Tokyo, Tokyo 113-8655, Japan
[2]Department of Metabolic Diseases, University of Tokyo, Faculty of Medicine, Tokyo 113-8655, Japan
[3]Department of Endocrinology & Nephrology, Faculty of Medicine, Faculty of Medicine, University of Tokyo, Tokyo 113-8655, Japan

Abstract Since interaction between bone and lipid metabolism has been suggested, this study investigated the regulation of bone metabolism by adiponectin, a representative adipokine, by analyzing deficient and overexpressing transgenic mice. We initially confirmed that adiponectin and its receptors were expressed in osteoblastic and osteoclastic cells, indicating that adiponectin can act on bone not only through an endocrine pathway as a hormone secreted from fat tissue, but also through an autocrine/paracrine pathway. There was no abnormality in bone mass or turnover of adiponectin-deficient (Ad−/−) mice, possibly due to an equivalent balance of the two pathways. In the culture of bone marrow cells from the Ad−/− mice, osteogenesis was decreased compared to the wild-type (WT) cell culture, indicating a positive effect of endogenous adiponectin through the autocrine/paracrine pathway. To examine the endocrine action of adiponectin, we analyzed transgenic mice overexpressing adiponectin in the liver, and found no abnormality in the bone. Addition of recombinant adiponectin in cultured osteoprogenitor cells suppressed osteogenesis, suggesting that the direct action of circulating adiponectin was negative for bone formation. In the presence of insulin, however, this suppression was blunted, and adiponectin enhanced the insulin-induced phosphorylations of the main downstream molecule insulin receptor substrate-1 and Akt. These lines of results suggest three distinct adiponectin actions on bone formation: a positive action through the autocrine/paracrine pathway by locally produced adiponectin, a negative action through the direct pathway by circulating adiponectin, and a positive action through the indirect pathway by circulating adiponectin via enhancement of the insulin signaling. J. Cell. Biochem. 99: 196–208, 2006.

Key words: adiponectin; adipokine; fat; osteoblast; bone

Adiponectin, also called Acrp30, apM1, and adipoQ, is a recently discovered adipokine that is synthesized and secreted mainly by fat tissue [Scherer et al., 1995; Hu et al., 1996; Maeda et al., 1996; Nakano et al., 1996]. It is a 244-amino acid protein structurally similar to tumor necrosis factor-α (TNF-α) with an N-terminal collagenous repeat and a C-terminal globular domain [Hu et al., 1996]. Although it is abundant in plasma, the level is reduced in association with obesity and obesity-linked diseases including type 2 diabetes, unlike most other adipokines including leptin, resistin, TNF-α, and interleukin-6 (IL-6) [Arita et al., 1999; Hotta et al., 2000; Weyer et al., 2001; Matsubara et al., 2002; Ukkola and Santaniemi, 2002]. Accumulated evidence has shown that adiponectin plays important roles in the regulation of insulin sensitivity, energy homeostasis, atherogenic changes of vessels, and inflammatory responses [Berg et al., 2001; Combs et al.,

Grant sponsor: Japanese Ministry of Education, Culture, Sports, Science, and Technology; Grant number: 17591551.
*Correspondence to: Hiroshi Kawaguchi, MD, PhD, Sensory & Motor System Medicine, Faculty of Medicine, University of Tokyo, Hongo 7-3-1, Bunkyo, Tokyo 113-8655, Japan. E-mail: kawaguchi-ort@h.u-tokyo.ac.jp
Received 12 January 2006; Accepted 16 February 2006
DOI 10.1002/jcb.20890

2001; Fruebis et al., 2001; Diez and Iglesias, 2003], indicating that adiponectin possesses potent functions in various tissues. Two adiponectin receptors, AdipoR1 and AdipoR2, were recently identified: the former is predominantly expressed in muscle whereas the latter in the liver [Yamauchi et al., 2003a]. Expression of both receptors has also been reported at high levels in human and rat pancreatic β cells, and their presence is suggested to be one mechanism for modulating the effects of circulating adiponectin [Kharroubi et al., 2003].

The low incidence of osteoporosis in obese people [Felson et al., 1993; Tremollieres et al., 1993], suggested a hypothesis whereby bone and adipose tissues would be controlled by the same hormone(s). Testing this hypothesis revealed that leptin, another representative adipokine regulating the fat mass, is a powerful inhibitor of bone formation by way of a sympathetic nerve system [Ducy et al., 2000; Takeda et al., 2002]. The adiponectin signal is also suggested to be involved in bone homeostasis since expressions of adiponectin, AdipoR1, and AdipoR2 were detected in human primary osteoblasts [Berner et al., 2004] and exogenous adiponectin has been reported to regulate osteoblast functions [Luo et al., 2005; Oshima et al., 2005]. A clinical study also showed that serum adiponectin was inversely associated with bone density [Lenchik et al., 2003]. Despite accumulation of evidence for adiponectin being a possible signal linking fat mass to bone mass, its physiological function on bone metabolism remains unclarified. Hence, the present study investigated the effects of gain and loss of functions of adiponectin on bone metabolism by analyzing adiponectin deficient and overexpressing transgenic mice.

MATERIALS AND METHODS

Animals

The adiponectin-deficient (Ad−/−) mice were generated and maintained as reported previously [Kubota et al., 2002]. In each analysis of Ad−/− mice, homozygous wild-type (WT) and Ad−/− male mice that were littermates generated from the intercross between heterozygous mice were compared. The transgenic (Ad-Tg) mice that overexpress the mouse globular adiponectin driven by the human serum amyloid P component (SAP) promoter, so that the adiponectin expression is limited to liver, were generated as described previously [Yamauchi et al., 2003b]. In each analysis of Ad-Tg mice, male Ad-Tg and WT littermates that were generated from the intercross between heterozygous mice were compared. All mice were kept in plastic cages under standard laboratory conditions with a 12-h dark, 12-h light cycle, a constant temperature of 23°C, and humidity of 48%. The mice were fed a standard rodent diet (CE-2; CLEA Japan, Inc.) containing 25.2% protein, 4.6% fat, 4.4% fiber, 6.5% ash, 3.44 kcal/g, 2.5 IU vitamin D_3/g, 1.09% calcium, and 0.93% phosphorus with water ad libitum. All experiments were performed on male mice at 8 weeks of age and were reviewed and approved by the Medical Animal Care and Use Committee of the University of Tokyo.

Expression Patterns of Adiponectin and its Receptors

Bone marrow cells were collected from long bones of 8-week-old WT mice. For isolation of osteoblasts, calvariae of neonatal WT and Ad−/− mice were digested for 10 min at 37°C in an enzyme solution containing 0.1% collagenase and 0.2% dispase five times, and cells isolated by the last four digestions were combined. For cells of osteoclastic lineage, we used the culture of macrophage colony-stimulating factor (M-CSF)-dependent bone marrow macrophages (M-BMMΦ) as reported previously [Kobayashi et al., 2000]. Briefly, bone marrow cells from WT and Ad−/− mice were seeded at a density of 3×10^5 cells/well in a 24-multi-well plate and cultured in αMEM (Invitrogen, Carlsbad, CA) containing 10% FBS (HyClone Laboratories, Inc., Logan, UT), with macrophage colony-stimulating factor (M-CSF; 100 ng/ml). After culturing for 3 days, adherent cells were isolated as M-BMMΦ and used as osteoclast precursors. For mature osteoclasts, M-BMMΦ were further cultured with M-CSF (100 ng/ml) and soluble receptor activator of nuclear factor κB ligand (RANKL; 100 ng/ml) for 3 days, and multi-nucleated cells were isolated. In addition to these primary cells, mouse bone marrow-derived stromal cell line ST2 cells (RIKEN Cell Bank, Tsukuba, Japan) were cultured in αMEM/10% FBS to subconfluency, and harvested. To investigate the expression of adiponectin and its receptors AdipoR1 and AdipoR2 in the bone cells above, RT-PCR was performed within an exponential phase of the amplification. An aliquot (1 μg) of total RNA extracted

using an ISOGEN kit (Wako Pure Chemical Industries, Ltd.) was reverse transcribed using Super Script reverse transcriptase (Takara Shuzo Co., Ltd., Shiga, Japan) with random hexamer (Takara Shuzo), and 5% of the reaction mixture was amplified with LA-Taq DNA polymerase (Takara Shuzo) using specific primer pairs: 5′-TGTTGCTGGGAGCTGTTCTACTG-3′ and 5′-ATGTCTCCCTTAGGACCAATAAG-3′ for adiponectin, 5′-GAAGACAGTGGGTA-CATGCGAATG-3′ and 5′-CCTCATGGAGGAA-GGCACTGCTG-3′ for AdipoR1, 5′-GCACCG-CCGAGATGGACTGCTGAA-3′ and 5′-GG-C-GGAAAGAGGATGGAGGTGACG-3′ for Adi-poR2, and 5′-CATGTAGGCCATGAGGTCCAC-CAC-3′ and 5′-TGAAGGTCGGTGTGAACGGA-TTTGGC-3′ for G3PDH. Up to 25 cycles of amplification were performed with a Perkin Elmer PCR Thermal Cycler (PE-2400; Perkin-Elmer Corp., Norwalk, CT) at 94°C for 30 sec, at 52–60°C for 60 sec, and at 72°C for 90 sec. As negative controls to exclude genomic amplification, total RNA without reverse transcription was directly used for PCR.

Analysis of Skeletal Morphology

A bone radiograph of whole bodies, femurs, and tibiae was taken with a soft X-ray apparatus (SOFTEX, CMB-2, Tokyo, Japan). Bone mineral density (BMD; mg/cm^2) of the right femurs, tibiae, and L2-L5 vertebral bodies were determined using dual-energy X-ray absorptiometry (DEXA) (PIXImus^{TM} Mouse Densitometer; Lunar Corp., Madison, WI), according to the manufacturer's instructions. All histological analyses were carried out using left tibiae of 8-week-old mice. For the assessment of dynamic histomorphometric indices, mice were injected subcutaneously with 8 mg/kg BW of calcein at 10 days and 3 days before sacrifice. After the sacrifice, the left tibiae were excised, fixed with ethanol, and the undecalcified bones were embedded in glycolmethacrylate. Three micrometers sagittal sections from the proximal parts of the tibiae were stained with Villanueva–Goldner and were visualized under fluorescent light microscopy for calcein labeling. The specimens were subjected to histomorphometric analyses using a semiautomated system (Osteoplan II; Carl Zeiss). Parameters for the trabecular bone were measured in an area 1.2 mm in length from 250 μm below the growth plate at the proximal metaphysis of the tibiae. Nomenclature, symbols, and units are those recommended by the Nomenclature Committee of the American Society for Bone and Mineral Research [Parfitt et al., 1987].

Bone Marrow Cell Cultures

Bone marrow cells were collected from long bones of 8-week-old WT and Ad−/− male littermates. Cells were plated at a density of 10^6 cells on a six-multi-well plate in αMEM containing 10% FBS, with 50 μg/ml ascorbic acid, and 10 mM β-glycerophosphate for osteogenesis assay, and with 1 μM troglitazone for the adipogenesis assay. For the alkaline phosphatase (ALP) staining, cultured plates were rinsed with PBS, fixed in 100% ethanol at 10 days of culture, and stained with Tris-HCl-buffered solution (pH 9.0) containing naphthol AS-MX phosphate as a substrate and Fast Blue BB salt (Sigma-Aldrich, St. Louis, MS) as a coupler. For the Alizarin red staining, cultured plates were rinsed with PBS at 21 days of culture, fixed in 10% buffered formalin, and stained with 2% Alizarin red S (pH 4.0) (Sigma-Aldrich). For the analysis of adipogenesis, the medium was supplemented with 1 μM troglitazone (Sankyo Pharmaceutical Co., Tokyo) for 10 days, fixed in 10 mM sodium periodate, 2% paraformaldehyde, 75 mM L-lysin dihydrochloride, and 37.5 mM sodium phosphate, and then stained in a filtered solution of 0.3% oil red O in 60% isopropanol for 15 min. The red-stained, lipid vacuole-containing cells in a well were counted.

Osteoclast Formation Assay

Tartrate resistant acid phosphatase (TRAP)-positive multi-nucleated osteoclasts were generated by coculturing bone marrow cells (5×10^5 cells/well) and calvarial osteoblasts (1×10^4 cells/well), derived from either WT or Ad−/− littermates, in a 24-multi-well plate for 6 days in αMEM containing 10% FBS and $1,25(OH)_2D_3$ (10 nM). The staining was performed at pH 5.0 in the presence of L(+)-tartaric acid using naphthol AS-MX phosphate (Sigma-Aldrich) in N, *N*-dimethyl formamide as the substrate. Cells positively stained for TRAP containing more than three nuclei were counted as osteoclasts.

Effects of Recombinant Adiponectin on Bone Marrow Cells and ST2 Cells

Recombinant mouse full-length adiponectin expressed in *Escherichia coli* was isolated and

purified as previously described [Yamauchi et al., 2003a]. Bone marrow cells collected from long bones of WT mice were plated at a density of 10^6 cells/well in a six-multi-well plate, cultured with 0, 3, and 10 μg/ml of recombinant adiponectin in αMEM/10% FBS/ascorbic acid/β-glycerophosphate in the presence and absence of insulin (10 nM), and stained with ALP and Alizarin red after 10 and 21 days, respectively, as described above. ST2 cells were inoculated at a density of 1×10^4 cells/well in a 24-multi-well plate, cultured with 0, 1, 3 and 10 μg/ml of recombinant adiponectin in αMEM/10% FBS/ascorbic acid with insulin-like growth factor-I (IGF-I, 100 nM) or bone morphogenetic protein-2 (BMP-2, 10 nM). At 7 days of culture, cells were sonicated in 10 mM Tris-HCl buffer (pH 8.0) containing 1 mM $MgCl_2$ and 0.5% Triton X-100. ALP activity in the lysate was measured using a Wako ALP kit (Wako Pure Chemical) and the protein content was determined using BCA protein assay reagent (Pierce Biotechnology, Rockford, IL).

Immunoprecipitation and Immunoblotting

For immunoprecipitation and immunoblotting, bone marrow cells collected from long bones of WT mice were plated at a density of 2×10^6 cells/well in a 6 cm dish and cultured for 10 days as described above. After 6 h of serum starvation, cells were cultured with or without 10 μg/ml of recombinant adiponectin for 24 h. Cells were then stimulated with insulin (100 nM) or the vehicle for 10 min, and lysed with TNE buffer (10 mM Tris-HCl, 150 mM NaCl, 1% NP-40, 1 mM EDTA, 10 mM NaF, 2 mM Na_3VO_4, 1 mM aminoethyl-benzenesulfonyl fluoride, and aprotinin). A part of the cell lysates (100 μg) were immunoprecipitated with an anti-insulin receptor substrate (IRS)-1 antibody (Upstate, Waltham, MA) conjugated to protein G-Sepharose (Invitrogen) overnight at 4°C. The cell lysates with or without the immunoprecipitation that contained an equivalent amount of protein (20 μg) were electrophoresed by 8% SDS–PAGE, and transferred to PVDF membrane. After blocking with 5% BSA solution, they were incubated with either anti-phosphotyrosine (clone 4G10), anti-mouse phospho-Akt (Ser 472), anti-mouse Akt, or anti-mouse IRS-1 antibody (all from Upstate). Immunoreactive bands were stained using the ECL chemiluminescence reaction (Amersham Co., Arlington Heights, IL).

Statistical Analysis

Means of groups were compared by ANOVA and significance of differences was determined by post hoc testing using Bonferroni's method.

RESULTS

Expressions of Adiponectin and its Receptors in Bone Cells

Because adiponectin and its two receptors AdipoR1 and AdipoR2 were reported to be differentially expressed in a variety of cells and tissues [Yamauchi et al., 2003a; Berner et al., 2004], we first investigated their expressions in cells of osteoblastic and osteoclastic lineages by RT-PCR (Fig. 1). All mRNA expressions were detected in bone marrow cells, calvarial osteoblasts, osteoclast precursor M-BMMΦ, and isolated mature osteoclasts that were derived from WT mice, suggesting that they are ubiquitously expressed in various

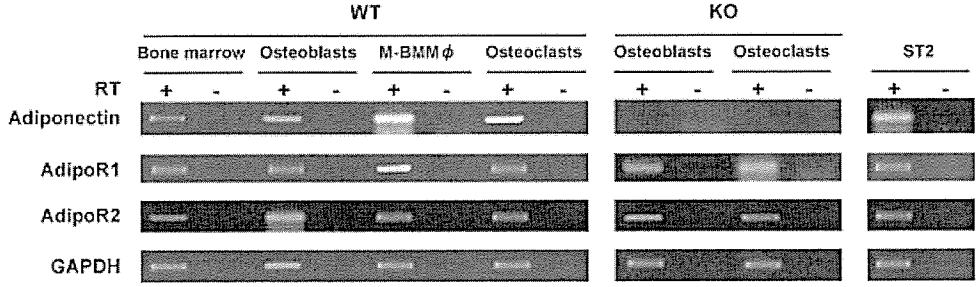

Fig. 1. Expressions of adiponectin and its receptors AdipoR1 and AdipoR2 in cells of osteoblastic and osteoclastic lineages derived from WT and Ad−/− mice by RT-PCR. Total RNA was extracted from bone marrow cells collected from adult mouse long bones, neonatal mouse calvarial osteoblasts, osteoclast precursor M-CSF-dependent bone marrow macrophages (M-BMMΦ), mature osteocalsts formed and isolated from the culture of M-BMMΦ with M-CSF and RANKL, and mouse bone marrow-derived stromal cell line ST2 cells. An aliquot of total RNA with (+) or without (−) reverse transcription (RT) was amplified using specific primers within an exponential phase of the amplification.

kinds of cells in bone. Although adiponectin was confirmed not to be expressed in the Ad−/− cells, AdipoR1, and AdipoR2 were detected in both osteoblasts and osteoclasts. In addition, all were also detected in a mouse stromal cell line ST2. These results indicate that adiponectin acts on bone not only through an endocrine pathway as a hormone secreted from fat tissue, but also through an autocrine/paracrine pathway. To elucidate the actions of adiponectin through these distinct pathways, we next performed experiments using the deficient and overexpressing transgenic mice.

No Abnormality in Bone of Adiponectin-Deficient Mice In Vivo

To examine the role of endogenous adiponectin in bone metabolism, we analyzed the bones of Ad−/− mice. Ad−/− mice developed and grew normally, indicating that adiponectin is not involved in the regulation of skeletal growth. X-ray analyses showed no significant difference in the skeleton between Ad−/− and WT littermates at 8 weeks of age (Fig. 2A). BMDs of the entire femurs, tibiae, and vertebrae (L2-L5) were also similar between mice of the two genotypes (Fig. 2B). In accordance with X-ray and BMD findings, histological analyses of the proximal tibiae of 8-week-old Ad−/− mice by the Villanueva–Goldner staining revealed no difference in bone phenotypes from those of WT littermates (Fig. 2C). The growth plate at the proximal tibiae of Ad−/− mice also seemed similar to that of WT, consistent with the lack of contribution of adiponectin to the skeletal growth. Bone histomorphometric measurements in this area supported these histological observations (Table I): there was no difference between Ad−/− and WT littermates in bone volume (BV/TV), bone formation parameters (Ob.S/BS & BFR), or bone resorption parameters (Oc.S/BS & ES/BS).

Suppression of Osteogenesis in the Culture of Adiponectin-Deficient Bone Marrow Cells

Considering that adiponectin acts through both endocrine and autocrine/paracrine pathways, the lack of abnormal phenotype in the bones of Ad−/− mice, which are not bone-specific conditional knockout mice but conventional knockout mice, may possibly be due to the equivalent balance of the two pathways. To examine the specific effect of the autocrine/paracrine action of adiponectin, in vitro cultures of bone marrow cells from Ad−/− and WT mice were compared. Surprisingly, osteogenesis determined by the number of colonies positively stained with ALP and Alizarin red was significantly decreased in the Ad−/− marrow cell culture as compared with that in the WT culture, suggesting a positive effect of the autocrine/paracrine action on bone formation (Fig. 3A, left and middle panels). However,

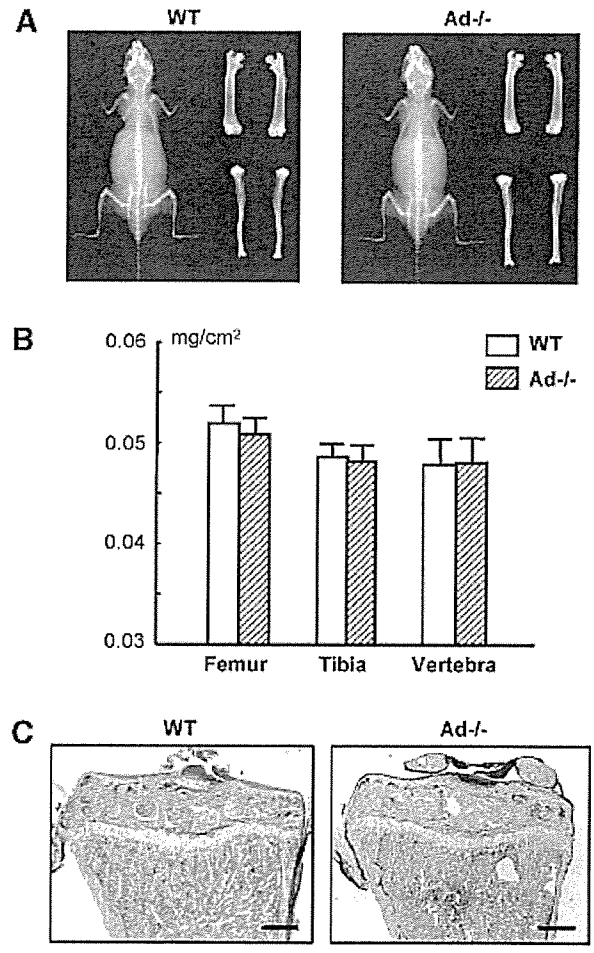

Fig. 2. Radiological and histological findings of the bones in male WT and Ad−/− littermates (8 weeks old). **A**: Plain X-ray images of the whole bodies (**left**), femurs (**upper right**), and tibiae (**lower right**) of representative WT and Ad−/− littermates. **B**: BMD of the entire femurs, tibiae, and L2-L5 vertebral bodies determined by DEXA. Data are expressed as means (bars) ± SEM (error bars) of 10 bones/group. None of the bones showed significant difference of BMD between the two genotypes. **C**: Histological features of the proximal tibiae of representative mice of each genotype. After the sacrifice, the tibiae were excised, fixed, embedded without decalcification, and the sagittal sections were stained with Villanueva–Goldner, in which mineralized bone was stained green and unmineralized osteoid red. Bar, 100 μm. Data of histomorphometric analyses are shown in Table I. [Color figure can be viewed in the online issue, which is available at www.interscience.wiley.com.]

TABLE I. Histomorphometry of Trabecular Bones in Proximal Tibiae of WT and Ad−/−Mice

	BV/TV (%)	Ob.S/BS (%)	BFR (mm^3/cm^2/year)	Oc.S/BS (%)	ES/BS (%)
WT	12.75 ± 0.96	11.93 ± 0.90	3.66 ± 0.92	4.58 ± 1.78	3.52 ± 0.79
Ad−/−	10.71 ± 1.92	12.07 ± 1.22	3.16 ± 0.93	4.32 ± 1.38	3.82 ± 0.89

Parameters for the trabecular bone were measured in an area 1.2 mm in length from 250 μm below the growth plate at the proximal metaphysis of the tibiae in Villanueva–Goldner and calcein double-labeled sections. Data expressed as means and standard errors (SEM) for 10 bones/group.
No significant difference of parameters between two genotypes (all $P > 0.05$).
BV/TV, trabecular bone volume expressed as a percentage of total tissue volume; Ob.S/BS, percentage of bone surface covered by cuboidal osteoblasts; BFR, bone formation rate; Oc.S/BS, percentage of bone surface covered by mature osteoclasts; ES/BS, percentage of eroded surface.

adipogenesis determined by the oil red O staining in the marrow cell culture was similar between Ad−/− and WT marrow cell cultures (Fig. 3A; right panel). To investigate the role of local adiponectin in osteoclastic cells, we next measured the number of TRAP-positive multinucleated osteoclasts formed in the coculture of bone marrow cells and primary osteoblasts, and found no difference between the cells of the two genotypes (Fig. 3B).

No Abnormality in Bone of Transgenic Mice Overexpressing Adiponectin in the Liver In Vivo

The in vivo Ad−/− bone analyses showed the equivalent balance of autocrine/paracrine and endocrine actions of adiponectin on bone (Fig. 2), while the in vitro Ad−/− marrow culture revealed the positive autocrine/paracrine action on bone formation (Fig. 3). These results imply a negative effect of circulating adiponectin on bone formation. Hence, we next examined the skeletal abnormality of transgenic mice overexpressing adiponectin (Ad-Tg) being driven by the SAP promoter, so that the adiponectin expression was limited to the liver and was not in the bone [Yamauchi et al., 2003b]. Ad-Tg mice appeared normal and indistinguishable from WT littermates in body weight and length. Plain X-ray images of Ad-Tg mice at 8 weeks showed no abnormality in the skeleton compared with WT littermates (Fig. 4A), and BMDs of the entire femurs, tibiae, and vertebrae (L2-L5) of Ad-Tg mice were also similar to those of WT littermates (Fig. 4B). Histological analyses of the proximal tibiae by the Villanueva–Goldner staining (Fig. 4C) and bone histomorphometric measurements (Table II) confirmed that neither the bone mass nor the bone turnover was affected by the circulating adiponectin.

Suppression of Osteogenesis by Recombinant Adiponectin in Osteoprogenitor Cell Cultures

We failed to detect the expected negative effect of circulating adiponectin on bone formation in Ad-Tg mice in vivo. However, since adiponectin is known to enhance the insulin action on its target organs [Berg et al., 2001; Combs et al., 2001; Fruebis et al., 2001; Yamauchi et al., 2001, 2003b; Kubota et al., 2002], the effect of circulating adiponectin on bone might partly be mediated by the insulin signaling that is anabolic for bone formation [Thomas et al., 1996]. Hence, we next looked at the systemic (or endocrine) action by examining the effect of addition of recombinant adiponectin on osteogenesis in cultures of osteoprogenitor cells in the presence and absence of insulin. In the cultures of bone marrow cells derived from WT long bones, osteogenesis determined by the numbers of colonies positively stained with ALP and Alizarin red were dose-dependently inhibited by recombinant adiponectin in the absence of insulin, indicating a direct/negative action of adiponectin on bone formation (Fig. 5A). However, in the presence of insulin (10 nM), the inhibition of osteogenesis by adiponectin was not seen in either ALP or Alizarin red staining. In the culture of mouse stromal cell line ST2, recombinant adiponectin also did not decrease ALP activity which was stimulated by IGF-I (100 nM), another bone anabolic factor that shares downstream molecules with the insulin signaling (Fig. 5B). In contrast, it dose-dependently decreased ALP activity which was stimulated by BMP-2 (10 nM).

We then investigated the effect of adiponectin on the intracellular signaling of insulin in bone marrow cells by examining the phosphorylations

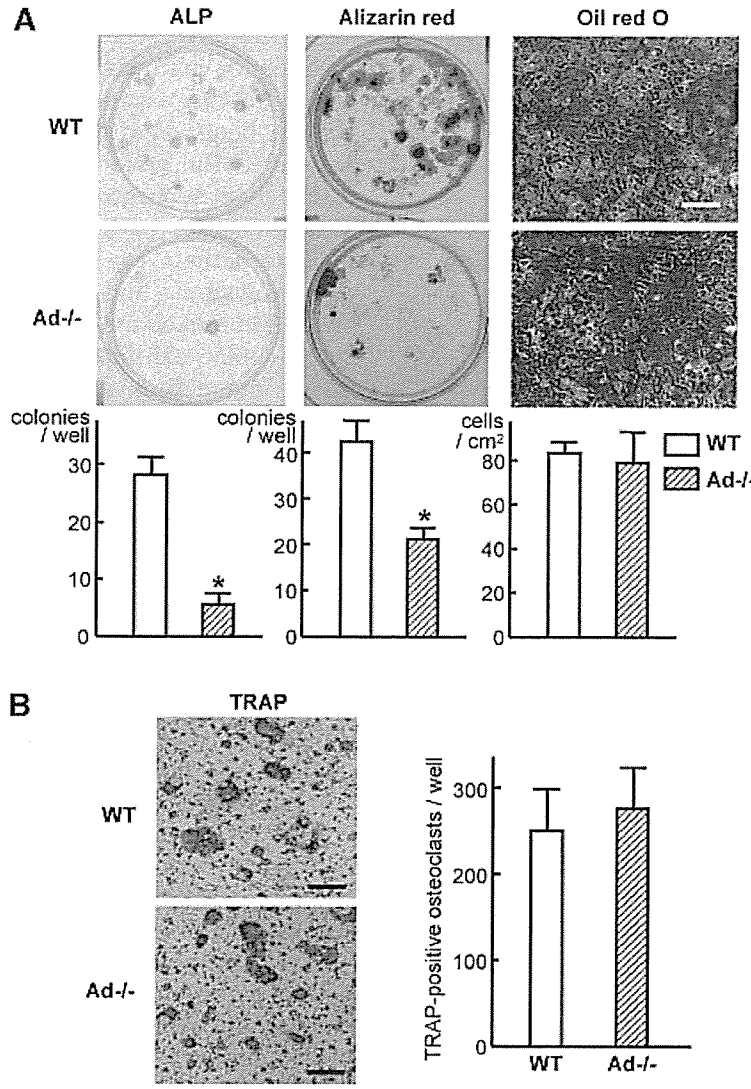

Fig. 3. Osteogenesis, adipogenesis, and osteoclastogenesis in cultures of bone marrow cells from WT and Ad−/− littermates. **A**: Osteogenesis was determined by ALP (**left**) and Alizarin red (**middle**) stainings of bone marrow cells cultured for 10 and 21 days, respectively, in αMEM/10% FBS with ascorbic acid and β-glycerophosphate. Adipogenesis was determined by oil red O staining (**right**) of bone marrow cells cultured for 10 days in αMEM/10% FBS with troglitazone. Bar, 200 μm. The graphs below indicate the number of positive colonies/well for ALP and Alizarin red stainings, and of positive cells/cm^2 for oil red O staining. Data are expressed as means (bars) ± SEMs (error bars) for eight wells/group. *, significant difference from the WT culture; $P < 0.01$. **B**: Osteoclastogensis was determined by the number of TRAP-positive multi-nucleated osteoclasts formed in the coculture of bone marrow cells and calvarial osteoblasts from WT and Ad−/− littermates in αMEM/10% FBS with $1,25(OH)_2D_3$ for 6 days. Bar, 400 μm. Data are expressed as mean (bars) ± SEM (error bars) for eight wells/group. There was no significant difference between WT and Ad−/− cultures. [Color figure can be viewed in the online issue, which is available at www.interscience.wiley.com.]

of IRS-1 and Akt, the main downstream molecules of insulin. Immunoprecipitation and immunoblotting analyses revealed that phosphorylations of IRS-1 and Akt were induced by insulin alone, while hardly being affected by recombinant adiponectin alone. More importantly, the phosphorylations induced by insulin were further enhanced by adiponectin, suggesting indirect/positive action of adiponectin on bone formation via enhancement of the insulin signaling (Fig. 5C).

The results indicate that no bone abnormality in Ad-Tg mice may be possibly due to an equivalent balance of the direct/negative and indirect/positive actions of circulating adiponectin. The direct action might possibly be related to the BMP signaling, and the indirect one may be through enhancement of the insulin signaling.

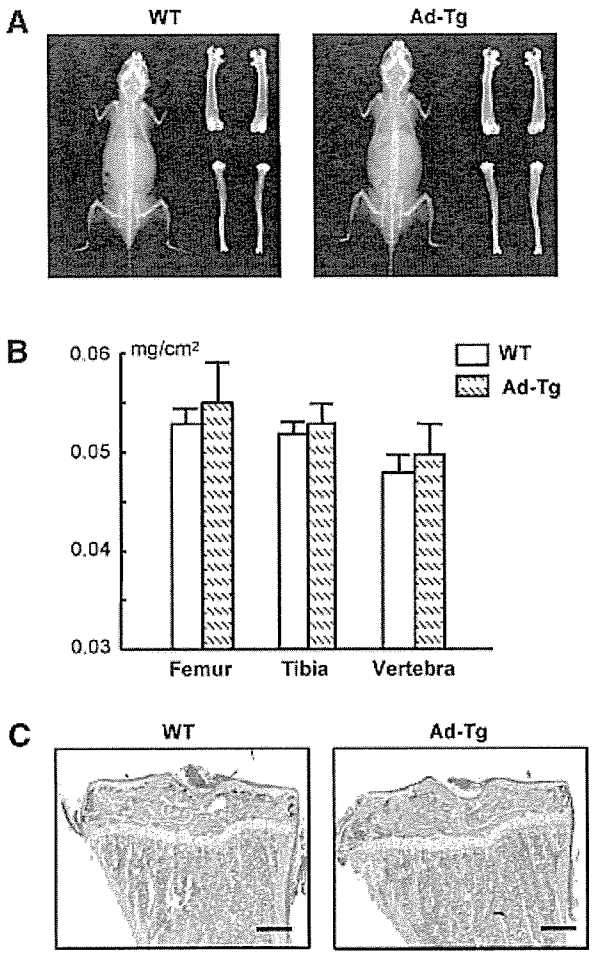

Fig. 4. Radiological and histological findings of the bones in male WT and Ad-Tg littermates (8 weeks old). **A:** Plain X-ray images of the whole bodies (**left**), femurs (**upper right**), and tibiae (**lower right**) of representative WT and Ad-Tg littermates. **B:** BMD of the entire femurs, tibiae, and L2-L5 vertebral bodies determined by DEXA. Data are expressed as means (bars) ± SEM (error bars) of 10 bones/group. None of the bones showed significant difference of BMD between the two genotypes. **C:** Histological features of the proximal tibiae of representative mice of the two genotypes prepared as described in Figure 2. Bar, 100 μm. Data of histomorphometric analyses are shown in Table II. [Color figure can be viewed in the online issue, which is available at www.interscience.wiley.com.]

DISCUSSION

Since we confirmed that adiponectin and its receptors were expressed not only in fat cells but also in bone cells (Fig. 1), the present study examined the actions of adiponectin on bone metabolism separately via autocrine/paracrine and endocrine pathways. To elucidate these distinct actions, we used several in vivo and in vitro systems, and found variable regulations of bone metabolism by adiponectin. First, the Ad−/− mice exhibited no abnormality in the bone, suggesting an equivalent balance of autocrine/paracrine and endocrine actions on bone (Fig. 2). Second, the in vitro adiponectin-deficient marrow cell culture revealed a potent osteogenic effect of adiponectin as an autocrine/paracrine factor (Fig. 3). Third, the lack of bone abnormality in the Ad-Tg mice indicated an equivalent balance of circulating adiponectin (Fig. 4). Lastly, recombinant adiponectin inhibited osteogenesis but enhanced the insulin signaling in osteoprogenitor cell cultures, suggesting the direct/negative and indirect/positive actions of circulating adiponectin on bone formation (Fig. 5). It is therefore speculated that there are at least three distinct adiponectin actions on bone formation: a positive action through the autocrine/paracrine pathway by locally produced adiponectin in bone, a negative action through the direct pathway by circulating adiponectin, and a positive action through the indirect pathway by circulating adiponectin via enhancement of the insulin signaling.

It is of note that effects of adiponectin on bone formation differed among experimental systems, that is, between in vivo and in vitro; between gain-of-function and loss-of-function. These discrepancies are also seen in the actions of leptin, another representative adipokine.

TABLE II. Histomorphometry of Trabecular Bones in Proximal Tibiae of WT and Ad-Tg Mice

	BV/TV (%)	Ob.S/BS (%)	BFR (mm^3/cm^2/year)	Oc.S/BS (%)	ES/BS (%)
WT	11.38 ± 0.67	10.38 ± 0.83	4.96 ± 0.62	5.49 ± 1.39	5.02 ± 0.90
Ad-Tg	13.97 ± 0.62	13.70 ± 1.01	5.06 ± 0.29	6.93 ± 1.87	4.42 ± 1.95

Parameters for the trabecular bone were measured in an area 1.2 mm in length from 250 mm below the growth plate at the proximal metaphysis of the tibiae in Villanueva–Goldner and calcein double-labeled sections. Data expressed as means and standard errors (SEM) for 10 bones/group.
No significant difference of parameters between two genotypes (all $P > 0.05$).
BV/TV, trabecular bone volume expressed as a percentage of total tissue volume; Ob.S/BS, percentage of bone surface covered by cuboidal osteoblasts; BFR, bone formation rate; Oc.S/BS, percentage of bone surface covered by mature osteoclasts; ES/BS, percentage of eroded surface.

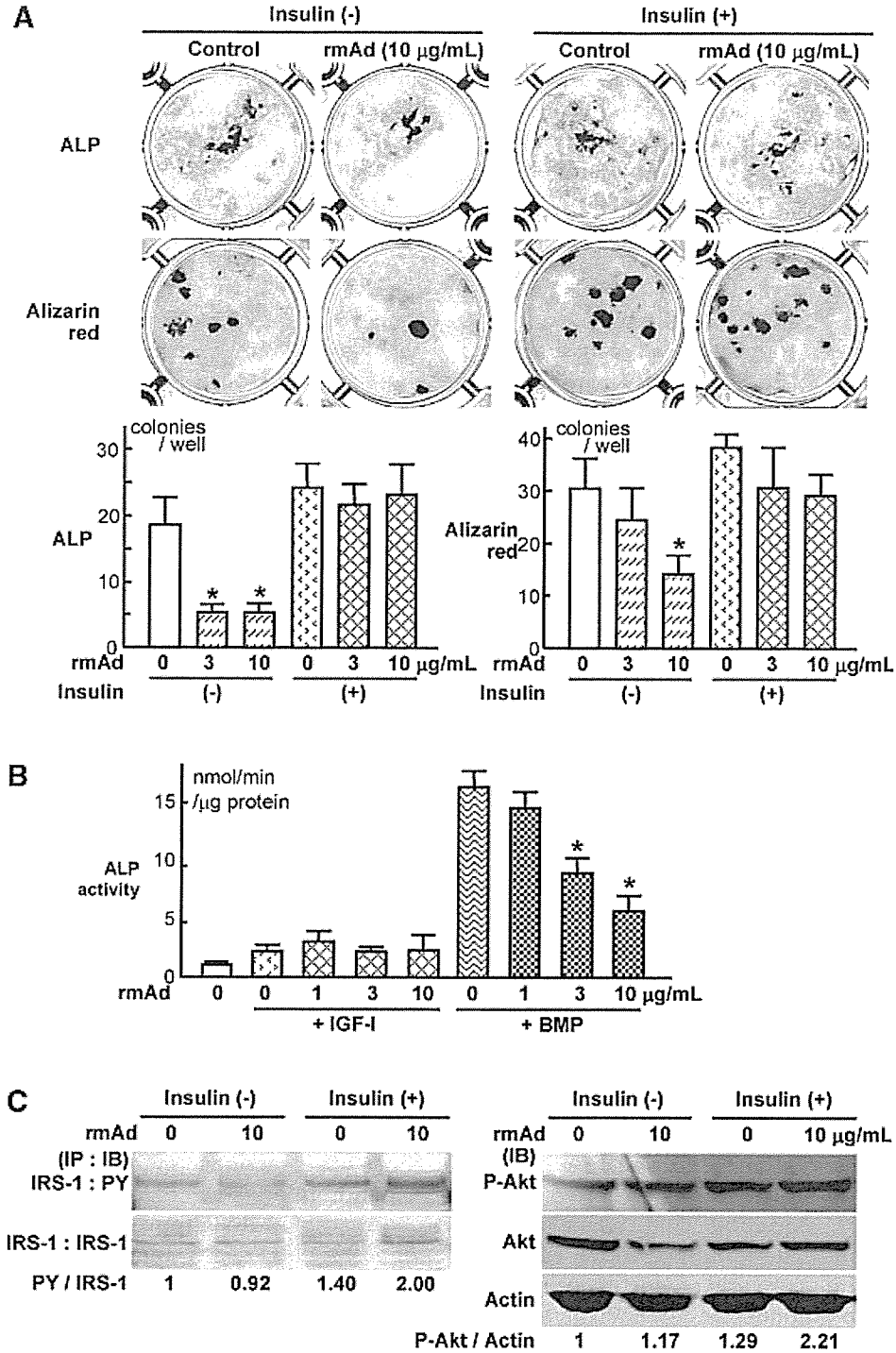

Fig. 5. **A**: Effect of recombinant mouse adiponectin (rmAd) on osteogenesis in the bone marrow cell culture. Osteogenesis was determined by ALP and Alizarin red stainings after 10 and 21 days of culture, respectively, with indicated concentrations of rmAd in αMEM/10% FBS/ascorbic acid/β-glycerophosphate with or without insulin (10 nM). The graphs below indicate the number of positive colonies/well. Data are expressed as means (bars) ± SEMs (error bars) for eight wells/group. *, significant inhibition by rmAd; $P < 0.01$. **B**: Effect of rmAd on ALP activity of ST2 cells cultured for 7 days with indicated concentrations of rmAd in αMEM/10% FBS/ascorbic acid and IGF-1(100 nM) or BMP-2 (10 nM). Data are expressed as means (bars) ± SEMs (error bars) for eight wells/group. *, significant inhibition by rmAd; $P < 0.01$. **C**: Effect of rmAd on phosphorylations of IRS-1 and Akt in cultured bone marrow cells. Protein levels of phosphorylated IRS-1, IRS-1, phosphorylated Akt, Akt, and β-actin were determined by immunoprecipitation (IP) and immunoblotting (IB) in the cells stimulated by insulin (100 nM) or the vehicle for 10 min after pre-treatment with or without rmAd (10 μg/ml) for 24 h. The number under each band shows the ratio of the band intensity of phosphorylated IRS-1 and phosphorylated Akt normalized to those of IRS-1 and β-actin, respectively, that were measured by densitometry. Similar results were obtained in five independent experiments. [Color figure can be viewed in the online issue, which is available at www.interscience.wiley.com.]

Leptin negatively regulates bone formation via a sympathetic nerve system in vivo [Ducy et al., 2000; Takeda et al., 2002; Elefteriou et al., 2004], while recombinant leptin induces osteogenesis in the culture of bone marrow stromal cells [Thomas et al., 1999]. This is implicated to be due to the existence of a circulating soluble leptin receptor that modulates the action of leptin [Kratzsch et al., 2002; Elefteriou et al., 2004]. Although neither soluble receptors nor binding proteins of adiponectin have been identified, it is possible that the co-factors might explain the diverse actions of adiponectin on bone. Another possible mechanism underlying the discrepancy may be a variety of adiponectin forms, since it is present as a full length or as cleavage products such as an active form C-terminal globular fragment in plasma [Fruebis et al., 2001; Kishida et al., 2003]. Although biological activities of the different forms of adiponectin are poorly understood, they might be specific for distinct receptors and cell types. Recently, Oshima et al. [2005] reported that a single injection of adenovirus expressing a full-length adiponectin increased bone mass by stimulating bone formation and suppressing bone resorption. In contrast, the present bone histomorphometric analysis of Ad-Tg mice with constitutive overexpression of the globular form of adiponectin revealed no abnormality in bone formation or bone resorption parameter. This difference may not be due to that of the molecular form since our preliminary investigation of the transgenic mice that overexpress the full-length adiponectin driven by the same SAP promoter also failed to show bone abnormality (unpublished observation by Yamauchi & Kadowaki). We therefore speculate that there may be a compensatory signaling that cancels the excessive adiponectin signaling, which cannot catch up with the acute and strong overexpression by a single adiponectin-adenovirus application.

The present in vitro experiments showed that recombinant full-length adiponectin at the physiological serum concentration (10 μg/ml) [Kubota et al., 2002] inhibited osteogenic differentiation from bone marrow cells and mouse stromal cell line ST2, which is also inconsistent with previous studies showing that it increased the differentiation and mineralization in the murine osteoblast cell line MC3T3-E1 cell and human primary osteoblast cultures [Luo et al., 2005; Oshima et al., 2005]. This might be due to the difference of differentiation stages of cells of osteoblastic lineage. The expression levels of AdipoR1 and AdipoR2 were similar in the precursor cells of the present study, while AdipoR1 was predominantly expressed in the more differentiated osteoblasts of the previous studies. Moreover, although this study implicated the involvement of the BMP pathway, earlier authors reported that the MAP kinase pathway is important for the adiponectin signaling [Luo et al., 2005]. In fact, our study using a mouse calvarial osteoblast culture failed to show the inhibitory effect of the recombinant adiponectin (data not shown). Another explanation for the discrepancy between the present and previous results may be the existence of other lineage of cells than osteoprogenitors in our culture systems, but not in the earlier systems. Because adiponectin is reported to variably regulate differentiation of bone marrow cells into several lineages through the ubiquitously expressed receptors, it is possible that adiponectin can affect other lineage of cells like lymphocytes and adipocytes, causing a proportional decrease of osteoprogenitors in bone marrow. It is known to inhibit B lymphopoiesis through induction of prostaglandin synthesis, but stimulates myelopoiesis [Yokota et al., 2003]. It also suppresses adipogenesis from bone marrow cells through a cyclooxygenase-2/prostaglandin-dependent mechanism [Yokota et al., 2002]; however, the present study showed normal adipogenesis from cultured Ad−/− marrow cells, suggesting the difference of actions of exogenous and endogenous adiponectin on adipogenic differentiation as well. Since the actions of prostaglandins differ depending on the concentration; high doses of prostaglandin suppress collagen synthesis whereas low doses induce it in osteoblasts [Chyun and Raisz, 1984], the actions of adiponectin on bone might be mediated in part by prostaglandin production, so that they differ depending on the concentration. Insofar as the effects of adiponectin on these other types of cells remain unclarified, we should acknowledge that the present study does not reach a definitive conclusion relating to the mechanism of adiponectin on bone homeostasis.

In addition to the direct and negative effect on the osteoprogenitor cells, circulating adiponectin exhibited a positive effect on bone formation through enhancement of the insulin signaling. There is a great deal of evidence supporting that

adiponectin increases the insulin action in its target organs. Recombinant adiponectin ameliorated insulin resistance in obese- and diabetic-KKA^y mice and diabetic-lipoatrophic mice, both of which had reduced plasma adiponectin levels [Yamauchi et al., 2001]. A single injection of recombinant adiponectin abolished hyperglycemia by suppressing glucose production in ob/ob, non-obese diabetic, or streptozotocin-treated mice [Berg et al., 2001; Combs et al., 2001]. Transgenic overexpression of adiponectin also ameliorated insulin resistance in ob/ob mice [Yamauchi et al., 2003b] and the disruption of the adiponectin gene is known to cause insulin resistance [Matsuzawa et al., 2004; Luo et al., 2005]. Another plausible hormone that might be related to the endocrine action of adiponectin might be estrogen, which is also a potent regulator of bone metabolism [Tanko and Christiansen, 2004]. A recent report demonstrated that estrogen can suppress adiponectin secretion in mice and cultured adipocytes [Combs et al., 2003], although the interactions of signalings among adiponectin, estradiol, and insulin in bone are complicated and remain to be further clarified [Kalish et al., 2003].

Regarding the clinical evidence of involvement of adiponectin in bone metabolism, Kontogianni et al. [2004] reported that the circulating level of adiponectin was not correlated with bone mass of perimenopausal women while that of leptin showed an inverse correlation. This is in accordance with the present results that both deficient and overexpressing transgenic mice of adiponectin showed normal bone mass. However, another clinical study by Lenchik et al. [2003] reported significant inverse correlations of adiponectin with visceral fat and BMD, and proposed adiponectin as a mediator of the protective effects of visceral fat mass on BMD. The correlations may be dependent on the balance of the direct and indirect actions of circulating adiponectin, which we showed oppositely affected bone metabolism. When we compare the populations of the two clinical studies above, more subjects (86%) in the study by Lenchik et al. were affected by type 2 diabetes than those in the study by Kontogianni et al. This might at least partly explain the discrepancy of the two clinical studies: in the former the indirect and positive effect of circulating adiponectin was suppressed due to the impaired insulin signaling, so that the direct and negative effect became predominant, while in the latter study there remained an equivalent balance between direct and indirect effects.

Adiponectin is structurally similar to TNF-α, receptor activator of nuclear factor κB ligand (RANKL) and osteoprotegerin, all of which are potent regulators of osteoclastogenesis [Ouchi et al., 2000; Tsao et al., 2002]. However, osteoclastogenesis from marrow cells was not affected by the deficiency of endogenous adiponectin (Ad−/−) in the present study, while a previous study showed a decrease of osteoclastogenesis by adiponectin in vivo and in vitro [Oshima et al., 2005]. This also indicates that there might be distinct effects of adiponectin on osteoclastogenesis through autocrine/paracrine and endocrine pathways. Considering that adiponectin expression is regulated by several bone regulators: it is reduced by TNF-α [Yokota et al., 2000], IL-6 [Kappes and Loffler, 2000], β-adrenergic agonists [Fasshauer et al., 2003], and glucocorticoids [Halleux et al., 2001], whereas stimulated by proliferator-activated receptor (PPARγ) agonists [Combs et al., 2002], adiponectin may play a role in the complicated molecular network that regulates bone metabolism.

ACKNOWLEDGMENTS

We thank Reiko Yamaguchi for providing expert technical assistance. Regrettably, Masayuki Yamaguchi died much young and before the publication of this study. We dedicate this study to him and his family. This work was supported by Grant-in-Aid for Scientific Research from the Japanese Ministry of Education, Culture, Sports, Science, and Technology Grant no. 17591551.

REFERENCES

Arita Y, Kihara S, Ouchi N, Takahashi M, Maeda K, Miyagawa J, Hotta K, Shimomura I, Nakamura T, Miyaoka K, Kuriyama H, Nishida M, Yamashita S, Okubo K, Matsubara K, Muraguchi M, Ohmoto Y, Funahashi T, Matsuzawa Y. 1999. Paradoxical decrease of an adipose-specific protein, adiponectin, in obesity. Biochem Biophys Res Commun 257:79–83.

Berg AH, Combs TP, Du X, Brownlee M, Scherer PE. 2001. The adipocyte-secreted protein Acrp30 enhances hepatic insulin action. Nat Med 7:947–953.

Berner HS, Lyngstadaas SP, Spahr A, Monjo M, Thommesen L, Drevon CA, Syversen U, Reseland JE. 2004. Adiponectin and its receptors are expressed in bone-forming cells. Bone 35:842–849.

Chyun YS, Raisz LG. 1984. Stimulation of bone formation by prostaglandin E2. Prostaglandins 27:97–103.

Combs TP, Berg AH, Obici S, Scherer PE, Rossetti L. 2001. Endogenous glucose production is inhibited by the adipose-derived protein Acrp30. J Clin Invest 108: 1875–1881.

Combs TP, Wagner JA, Berger J, Doebber T, Wang WJ, Zhang BB, Tanen M, Berg AH, O'Rahilly S, Savage DB, Chatterjee K, Weiss S, Larson PJ, Gottesdiener KM, Gertz BJ, Charron MJ, Scherer PE, Moller DE. 2002. Induction of adipocyte complement-related protein of 30 kilodaltons by PPARgamma agonists: A potential mechanism of insulin sensitization. Endocrinology 143: 998–1007.

Combs TP, Berg AH, Rajala MW, Klebanov S, Iyengar P, Jimenez-Chillaron JC, Patti ME, Klein SL, Weinstein RS, Scherer PE. 2003. Sexual differentiation, pregnancy, calorie restriction, and aging affect the adipocyte-specific secretory protein adiponectin. Diabetes 52:268–276.

Diez JJ, Iglesias P. 2003. The role of the novel adipocyte-derived hormone adiponectin in human disease. Eur J Endocrinol 148:293–300.

Ducy P, Amling M, Takeda S, Priemel M, Schilling AF, Beil FT, Shen J, Vinson C, Rueger JM, Karsenty G. 2000. Leptin inhibits bone formation through a hypothalamic relay: A central control of bone mass. Cell 100:197–207.

Elefteriou F, Takeda S, Ebihara K, Magre J, Patano N, Kim CA, Ogawa Y, Liu X, Ware SM, Craigen WJ, Robert JJ, Vinson C, Nakao K, Capeau J, Karsenty G. 2004. Serum leptin level is a regulator of bone mass. Proc Natl Acad Sci USA 101:3258–3263.

Fasshauer M, Kralisch S, Klier M, Lossner U, Bluher M, Klein J, Paschke R. 2003. Adiponectin gene expression and secretion is inhibited by interleukin-6 in 3T3-L1 adipocytes. Biochem Biophys Res Commun 301:1045–1050.

Felson DT, Zhang Y, Hannan MT, Anderson JJ. 1993. Effects of weight and body mass index on bone mineral density in men and women: The Framingham study. J Bone Miner Res 8:567–573.

Fruebis J, Tsao TS, Javorschi S, Ebbets-Reed D, Erickson MR, Yen FT, Bihain BE, Lodish HF. 2001. Proteolytic cleavage product of 30-kDa adipocyte complement-related protein increases fatty acid oxidation in muscle and causes weight loss in mice. Proc Natl Acad Sci USA 98:2005–2010.

Halleux CM, Takahashi M, Delporte ML, Detry R, Funahashi T, Matsuzawa Y, Brichard SM. 2001. Secretion of adiponectin and regulation of apM1 gene expression in human visceral adipose tissue. Biochem Biophys Res Commun 288:1102–1107.

Hotta K, Funahashi T, Arita Y, Takahashi M, Matsuda M, Okamoto Y, Iwahashi H, Kuriyama H, Ouchi N, Maeda K, Nishida M, Kihara S, Sakai N, Nakajima T, Hasegawa K, Muraguchi M, Ohmoto Y, Nakamura T, Yamashita S, Hanafusa T, Matsuzawa Y. 2000. Plasma concentrations of a novel, adipose-specific protein, adiponectin, in type 2 diabetic patients. Arterioscler Thromb Vasc Biol 20: 1595–1599.

Hu E, Liang P, Spiegelman BM. 1996. AdipoQ is a novel adipose-specific gene dysregulated in obesity. J Biol Chem 271:10697–10703.

Kalish GM, Barrett-Connor E, Laughlin GA, Gulanski BI. 2003. Association of endogenous sex hormones and insulin resistance among postmenopausal women: Results from the postmenopausal estrogen/progestin intervention trial. J Clin Endocrinol Metab 88:1646–1652.

Kappes A, Loffler G. 2000. Influences of ionomycin, dibutyryl-cycloAMP and tumour necrosis factor-alpha on intracellular amount and secretion of apM1 in differentiating primary human preadipocytes. Horm Metab Res 32:548–554.

Kharroubi I, Rasschaert J, Eizirik DL, Cnop M. 2003. Expression of adiponectin receptors in pancreatic beta cells. Biochem Biophys Res Commun 312:1118–1122.

Kishida K, Nagaretani H, Kondo H, Kobayashi H, Tanaka S, Maeda N, Nagasawa A, Hibuse T, Ohashi K, Kumada M, Nishizawa H, Okamoto Y, Ouchi N, Maeda K, Kihara S, Funahashi T, Matsuzawa Y. 2003. Disturbed secretion of mutant adiponectin associated with the metabolic syndrome. Biochem Biophys Res Commun 306:286–292.

Kobayashi K, Takahashi N, Jimi E, Udagawa N, Takami M, Kotake S, Nakagawa N, Kinosaki M, Yamaguchi K, Shima N, Yasuda H, Morinaga T, Higashio K, Martin TJ, Suda T. 2000. Tumor necrosis factor alpha stimulates osteoclast differentiation by a mechanism independent of the ODF/RANKL-RANK interaction. J Exp Med 191: 275–286.

Kontogianni MD, Dafni UG, Routsias JG, Skopouli FN. 2004. Blood leptin and adiponectin as possible mediators of the relation between fat mass and BMD in perimenopausal women. J Bone Miner Res 19:546–551.

Kratzsch J, Lammert A, Bottner A, Seidel B, Mueller G, Thiery J, Hebebrand J, Kiess W. 2002. Circulating soluble leptin receptor and free leptin index during childhood, puberty, and adolescence. J Clin Endocrinol Metab 87:4587–4594.

Kubota N, Terauchi Y, Yamauchi T, Kubota T, Moroi M, Matsui J, Eto K, Yamashita T, Kamon J, Satoh H, Yano W, Froguel P, Nagai R, Kimura S, Kadowaki T, Noda T. 2002. Disruption of adiponectin causes insulin resistance and neointimal formation. J Biol Chem 277:25863–25866.

Lenchik L, Register TC, Hsu FC, Lohman K, Nicklas BJ, Freedman BI, Langefeld CD, Carr JJ, Bowden DW. 2003. Adiponectin as a novel determinant of bone mineral density and visceral fat. Bone 33:646–651.

Luo XH, Guo LJ, Yuan LQ, Xie H, Zhou HD, Wu XP, Liao EY. 2005. Adiponectin stimulates human osteoblasts proliferation and differentiation via the MAPK signaling pathway. Exp Cell Res 309:99–109.

Maeda K, Okubo K, Shimomura I, Funahashi T, Matsuzawa Y, Matsubara K. 1996. cDNA cloning and expression of a novel adipose specific collagen-like factor, apM1 (AdiPose Most abundant Gene transcript 1). Biochem Biophys Res Commun 221:286–289.

Matsubara M, Maruoka S, Katayose S. 2002. Inverse relationship between plasma adiponectin and leptin concentrations in normal-weight and obese women. Eur J Endocrinol 147:173–180.

Matsuzawa Y, Funahashi T, Kihara S, Shimomura I. 2004. Adiponectin and metabolic syndrome. Arterioscler Thromb Vasc Biol 24:29–33.

Nakano Y, Tobe T, Choi-Miura NH, Mazda T, Tomita M. 1996. Isolation and characterization of GBP28, a novel gelatin-binding protein purified from human plasma. J Biochem (Tokyo) 120:803–812.

Oshima K, Nampei A, Matsuda M, Iwaki M, Fukuhara A, Hashimoto J, Yoshikawa H, Shimomura I. 2005. Adiponectin increases bone mass by suppressing osteoclast and activating osteoblast. Biochem Biophys Res Commun 331:520–526.

Ouchi N, Kihara S, Arita Y, Okamoto Y, Maeda K, Kuriyama H, Hotta K, Nishida M, Takahashi M, Muraguchi M, Ohmoto Y, Nakamura T, Yamashita S, Funahashi T, Matsuzawa Y. 2000. Adiponectin, an adipocyte-derived plasma protein, inhibits endothelial NF-kappaB signaling through a cAMP-dependent pathway. Circulation 102:1296–1301.

Parfitt AM, Drezner MK, Glorieux FH, Kanis JA, Malluche H, Meunier PJ, Ott SM, Recker RR. 1987. Bone histomorphometry: Standardization of nomenclature, symbols, and units. Report of the ASBMR Histomorphometry Nomenclature Committee. J Bone Miner Res 2: 595–610.

Scherer PE, Williams S, Fogliano M, Baldini G, Lodish HF. 1995. A novel serum protein similar to C1q, produced exclusively in adipocytes. J Biol Chem 270:26746–26749.

Takeda S, Elefteriou F, Levasseur R, Liu X, Zhao L, Parker KL, Armstrong D, Ducy P, Karsenty G. 2002. Leptin regulates bone formation via the sympathetic nervous system. Cell 111:305–317.

Tanko LB, Christiansen C. 2004. Can confounding with fat-derived endogenous free estradiol explain the inverse correlation of bone mineral density with adiponectin? Bone 34:916; author reply 917.

Thomas DM, Hards DK, Rogers SD, Ng KW, Best JD. 1996. Insulin receptor expression in bone. J Bone Miner Res 11:1312–1320.

Thomas T, Gori F, Khosla S, Jensen MD, Burguera B, Riggs BL. 1999. Leptin acts on human marrow stromal cells to enhance differentiation to osteoblasts and to inhibit differentiation to adipocytes. Endocrinology 140:1630–1638.

Tremollieres FA, Pouilles JM, Ribot C. 1993. Vertebral postmenopausal bone loss is reduced in overweight women: A longitudinal study in 155 early postmenopausal women. J Clin Endocrinol Metab 77:683–686.

Tsao TS, Murrey HE, Hug C, Lee DH, Lodish HF. 2002. Oligomerization state-dependent activation of NF-kappa B signaling pathway by adipocyte complement-related protein of 30 kDa (Acrp30). J Biol Chem 277:29359–29362.

Ukkola O, Santaniemi M. 2002. Adiponectin: A link between excess adiposity and associated comorbidities? J Mol Med 80:696–702.

Weyer C, Funahashi T, Tanaka S, Hotta K, Matsuzawa Y, Pratley RE, Tataranni PA. 2001. Hypoadiponectinemia in obesity and type 2 diabetes: Close association with insulin resistance and hyperinsulinemia. J Clin Endocrinol Metab 86:1930–1935.

Yamauchi T, Kamon J, Waki H, Terauchi Y, Kubota N, Hara K, Mori Y, Ide T, Murakami K, Tsuboyama-Kasaoka N, Ezaki O, Akanuma Y, Gavrilova O, Vinson C, Reitman ML, Kagechika H, Shudo K, Yoda M, Nakano Y, Tobe K, Nagai R, Kimura S, Tomita M, Froguel P, Kadowaki T. 2001. The fat-derived hormone adiponectin reverses insulin resistance associated with both lipoatrophy and obesity. Nat Med 7:941–946.

Yamauchi T, Kamon J, Ito Y, Tsuchida A, Yokomizo T, Kita S, Sugiyama T, Miyagishi M, Hara K, Tsunoda M, Murakami K, Ohteki T, Uchida S, Takekawa S, Waki H, Tsuno NH, Shibata Y, Terauchi Y, Froguel P, Tobe K, Koyasu S, Taira K, Kitamura T, Shimizu T, Nagai R, Kadowaki T. 2003a. Cloning of adiponectin receptors that mediate antidiabetic metabolic effects. Nature 423:762–769.

Yamauchi T, Kamon J, Waki H, Imai Y, Shimozawa N, Hioki K, Uchida S, Ito Y, Takakuwa K, Matsui J, Takata M, Eto K, Terauchi Y, Komeda K, Tsunoda M, Murakami K, Ohnishi Y, Naitoh T, Yamamura K, Ueyama Y, Froguel P, Kimura S, Nagai R, Kadowaki T. 2003b. Globular adiponectin protected ob/ob mice from diabetes and ApoE-deficient mice from atherosclerosis. J Biol Chem 278:2461–2468.

Yokota T, Oritani K, Takahashi I, Ishikawa J, Matsuyama A, Ouchi N, Kihara S, Funahashi T, Tenner AJ, Tomiyama Y, Matsuzawa Y. 2000. Adiponectin, a new member of the family of soluble defense collagens, negatively regulates the growth of myelomonocytic progenitors and the functions of macrophages. Blood 96:1723–1732.

Yokota T, Meka CS, Medina KL, Igarashi H, Comp PC, Takahashi M, Nishida M, Oritani K, Miyagawa J, Funahashi T, Tomiyama Y, Matsuzawa Y, Kincade PW. 2002. Paracrine regulation of fat cell formation in bone marrow cultures via adiponectin and prostaglandins. J Clin Invest 109:1303–1310.

Yokota T, Meka CS, Kouro T, Medina KL, Igarashi H, Takahashi M, Oritani K, Funahashi T, Tomiyama Y, Matsuzawa Y, Kincade PW. 2003. Adiponectin, a fat cell product, influences the earliest lymphocyte precursors in bone marrow cultures by activation of the cyclooxygenase-prostaglandin pathway in stromal cells. J Immunol 171:5091–5099.

Cartilage tissue engineering using human auricular chondrocytes embedded in different hydrogel materials

Hisayo Yamaoka,[1,2] Hirotaka Asato,[2] Toru Ogasawara,[1,3] Satoru Nishizawa,[1] Tsuguharu Takahashi,[1] Takashi Nakatsuka,[4] Isao Koshima,[2] Kozo Nakamura,[5] Hiroshi Kawaguchi,[5] Ung-il Chung,[3] Tsuyoshi Takato,[3,6] Kazuto Hoshi[1,3]

[1]*Department of Fujisoft ABC Cartilage and Bone Regeneration, Graduate School of Medicine, The University of Tokyo, Hongo 7–3-1, Bunkyo-Ku, Tokyo 113-0033, Japan*

[2]*Department of Plastic and Reconstructive Surgery, Graduate School of Medicine, The University of Tokyo, Hongo 7–3-1, Bunkyo-Ku, Tokyo 113-0033, Japan*

[3]*Division of Tissue Engineering, Faculty of Medicine, The University of Tokyo, Hongo 7–3-1, Bunkyo-Ku, Tokyo 113-0033, Japan*

[4]*Department of Plastic and Reconstructive Surgery, Saitama Medical School, Morohongo 38, Moroyama-machi, Iruma-gun, Saitama 350-0495, Japan*

[5]*Department of Orthopaedic Surgery, Graduate School of Medicine, The University of Tokyo, Hongo 7–3-1, Bunkyo-Ku, Tokyo 113-0033, Japan*

[6]*Department of Oral and Maxillofacial Surgery, Graduate School of Medicine, The University of Tokyo, Hongo 7–3-1, Bunkyo-Ku, Tokyo 113-0033, Japan*

Received 25 February 2005; revised 29 June 2005; accepted 12 July 2005
Published online 4 April 2006 in Wiley InterScience (www.interscience.wiley.com). DOI: 10.1002/jbm.a.30655

Abstract: To seek a suitable scaffold for cartilage tissue engineering, we compared various hydrogel materials originating from animals, plants, or synthetic peptides. Human auricular chondrocytes were embedded in atelopeptide collagen, alginate, or PuraMatrix™, all of which are or will soon be clinically available. The chondrocytes in the atelopeptide collagen proliferated well, while the others showed no proliferation. A high-cell density culture within each hydrogel enhanced the expression of collagen type II mRNA, when compared with that without hydrogel. By stimulation with insulin and BMP-2, collagen type II and glycosaminoglycan were significantly accumulated within all hydrogels. Chondrocytes in the atelopeptide collagen showed high expression of β1 integrin, seemingly promoting cell–matrix signaling. The N-cadherin expression was inhibited in the alginate, implying that decrease in cell-to-cell contacts may maintain chondrocyte activity. The matrix synthesis in PuraMatrix™ was less than that in others, while its Young's modulus was the lowest, suggesting a weakness in gelling ability and storage of cells and matrices. Considering biological effects and clinical availability, atelopeptide collagen may be accessible for clinical use. However, because synthetic peptides can control the risk of disease transmission and immunoreactivities, some improvement in gelling ability would provide a more useful hydrogel for ideal cartilage regeneration. © 2006 Wiley Periodicals, Inc. J Biomed Mater Res 78A: 1–11, 2006

Key words: chondrocyte; scaffold; hydrogel; regenerative medicine; matrix

INTRODUCTION

Tissue engineering has been researched and developed to aid in the repair or reconstruction of defective or injured organs. In tissue engineering, the artificial tissues are composed of living cells, often with a suitable scaffold. The scaffold provides the seeded cells with the space for function and supports their activities. Because every scaffold possesses specific properties that fit some kinds of cells or mimic other tissues in mechanical strength, we should choose the optimal scaffold based on the characteristics of the target cells and tissues.

Cartilage is one of the expectative targets for tissue engineering, because cartilage differs from other tissues in its limited capacity for self-repair.[1] The difficulty in the self-repair of cartilage seems to be due to the lack of a sufficient supply of healthy chondrocytes to the defective sites or to the low productivity of matrices in regenerated chondrocytes. Cartilage tissue engineering could overcome such limitations by using

Correspondence to: K. Hoshi, M.D., Ph.D.; e-mail: pochitky@umin.ac.jp

ex vivo culture techniques and supportive artificial materials.

In principle, chondrocyte activities are maintained when they are placed in the proper 3D environment. During the development and growth of cartilage, the chondrocytes produce abundant matrices, encase themselves within cavities, and are eventually separated from each other.[2] In contrast, the chondrocytes deviated from the physiological 3D environment rapidly lose the typical phenotype and protein synthesis, which is termed dedifferentiation.[3] In cartilage tissue engineering, the chondrocytes isolated from their original tissues would be conditioned in a 3D environment, mimicking the physiological situation with favorable scaffolds so as to reproduce their functions and enhance protein synthesis.

To date, attempts have been made to use two types of scaffolds for cartilage tissue engineering. The first is a solid type of scaffold including a honeycomb, porous body, mesh, sponge, and unwoven fabric.[4] The solid-type scaffolds have some advantages in shaping the macroscopic structure of regenerated tissues or in supporting their mechanical strength. However, the use of solid-type scaffolds includes practical conflicts. The smaller the pore sizes are, the more difficult it will be for the cell suspension to infiltrate into the scaffold. In contrast, when the pore sizes of solid scaffolds are increased, the chondrocytes are attached to the walls of huge pores, but they are not placed in a 3D condition.

The second is a hydrogel. Various materials derived from animals or plants, for example, collagen type I gel,[5] atelopeptides of collagen,[6] fibrin glue,[7] gelatin,[8] agarose,[9] or alginate,[10,11] are classified as this type. Although the hydrogel lacks mechanical strength in itself, this type of material can be mixed with cells and can surround the seeded cells in all directions. The hydrogel type of scaffold could be used to reconstruct the 3D environment for the chondrocytes in cartilage tissue engineering. Many previous articles reported that those hydrogel materials were more effective in retaining chondrocyte functions or promoting matrix synthesis, when compared with monolayer culture.[6,9,12] However, the biological specificities of each hydrogel materials have seldom been compared with each other. Van Susante and coworkers compared the potentials of both collagen type I and alginate gels as carriers for bovine articular chondrocytes, and evaluated the proliferation and proteoglycan synthesis of chondrocytes when the cells were cultured in an encapsulation with each gel in media containing 10% fetus bovine serum. The collagen type I gel had promoted chondrocyte proliferation, but the alginate gel had an advantage in proteoglycan synthesis.[13] Because this collagen type I gel had been prepared in extraction with acetic acid,[5] it preserved some telopeptides of collagen and antigenicity. At present, atelopeptides of collagen that were treated with protease have been regarded to show even lower immunogenicity than does native collagen that has usually been used as a medical device for treatment of tissue defects or tissue engineering.[14]

In the present study, we selected some kinds of hydrogel scaffolds that are or will soon be clinically available, and examined proliferation and matrix synthesis of human chondrocytes in the encapsulation with them so as to provide information on the choice of a suitable scaffold for clinical application. We focused on atelopeptides of collagen and alginate, both of which have been used as materials for medical devices, and either of which is a typical hydrogel material derived from animals or plants. Because the atelopeptide collagen spontaneously polymerizes into a stable gel at neutral pH and physiological temperature, and because the alginate undergoes instant ionotrophic gelation in the presence of divalent cations such as Ca^{2+}, they are widely used for the 3D culture studies of chondrocytes.[6,10]

In addition to both materials derived from animals or plants, synthetic peptides were also evaluated as a potential candidate for a clinically-available hydrogel scaffold. The synthetic peptides, PuraMatrix™, have been recently designed to serve as substrates for cell growth, differentiation, and biological functions. PuraMatrix™ is composed of synthetic polypeptides ($AcN\text{-}(RADA)_4\text{-}CNH_2$).[15] The motif RAD was incorporated to mimic the known cell adhesion motif RGD that is found in many ECM proteins.[16] They assemble to form an *in vivo*-like 3D extracellular matrix hydrogel around 37°C at pH 7, suggesting characteristics similar to the atelopeptide collagen. This has been used for research on hepatic regeneration or nerve regeneration and has been reported to promote neurite outgrowth and synaptic formation in neural cells, as well as functional differentiation in hepatocyte-like cells.[15,17] At present, clinical trials of the PuraMatrix™ for use in the orthopedic field have been planned by the suppliers.

As the experimental design, human auricular chondrocytes were embedded within each hydrogel material at the identical concentration of 0.5% by weight. We examined the proliferation ability of the chondrocytes at Passage 2, which should be more expanded when large sizes of engineered tissues would be made. The cell/hydrogel constructs at low cell density (2×10^4 cells/mL) were incubated in a medium containing 10% fetal bovine serum (FBS). To evaluate matrix synthesis, we used the dedifferentiated chondrocytes of Passage 4, and made cell/hydrogel constructs at high cell density (10^7 cells/mL). The constructs were incubated with BMP-2 and insulin, either of which was reported to induce the redifferentiation of chondrocytes or effectively enhance matrix synthesis.[18,19] The properties of hydrogel or cell/hydrogel constructs

were examined cytologically, biochemically, histologically, and biomechanically. Moreover, to clarify the molecular effects of each hydrogel material, cell–matrix interactions or cell-to-cell contacts were examined through the gene expression pattern of β1 integrin or N-cadherin, both of which are major adhesion molecules in chondrocytes or their progenitors.[20,21]

MATERIALS AND METHODS

Chemicals and antibodies

Dulbecco's Modified Eagle's Medium Nutrient Mixture F-12 HAM (DMEM/F12), penicillin–streptomycin solution, and trypsin–EDTA solution were purchased from Sigma Chemical Co. (St. Louis, MO). Collagenase from *Clostridium histolyticum* and Isogen were from Wako Pure Chemical Industries (Osaka, Japan). Bullet kit chondrocyte growth medium (CGM) and sodium alginate were obtained from Cambrex Bioscience Walkersville (Walkersville, MD). Other reagents were atelopeptide collagen (Kawaken Fine Chemicals Co., Tokyo, Japan), fetal bovine serum (FBS, Thermo Electron, Melbourne, Australia), insulin (MP Biomedicals, Irvine, CA), OCT compound (Miles, Elkhart, IN), PuraMatrix™ (3DM, Cambridge, MA), and recombinant human bone morphogenetic protein-2 (BMP-2, kindly provided by Yamanouchi Pharmaceutical Co., Tokyo, Japan).

Chondrocyte isolation and preparation

All procedures for the present experiments were approved by the ethics committee of the University of Tokyo Hospital (ethics permission #622). With 0.15% collagenase digestion, human chondrocytes were isolated from remnant auricular cartilage of microtia patients who underwent the operation at the University of Tokyo Hospital, with informed consent. Isolated chondrocytes were seeded in a 100-mm plastic tissue culture dish at a density of 6400 cells/cm^2 and cultured in the CGM, in a 37°C/5% CO_2 incubator. The medium was changed three times per week. Passages were performed by treatment with trypsin-EDTA solution when the cells were approaching confluence.

Chondrocyte proliferation in each hydrogel

For the collagen-based 3D culture, chondrocytes (Passage 2) were suspended in 0.5% atelopeptide collagen solution (pH 7). The mixture was placed in each well of a six-well plate at 2 mL at a density of 2×10^4 cells/mL. The collagen formed a gel on 1 h incubation at 37°C, embedding the cells in a 3D condition (total 4×10^4 cells in 2 mL of gel). The medium containing DMEM/F-12 with or without 10% FBS was gently poured on the gel at a volume of 2 mL in a 37°C/5% CO_2 incubator. Throughout the experiment, the medium was changed three times per week. To release the cells, the gel was incubated in 0.3% collagenase at 37°C for 30 min.

In the case of alginate, chondrocytes (Passage 2) were resuspended in 0.5% sodium alginate. Two ml of the cell/alginate suspension at a density of 2×10^4 cells/mL was dropped into each well of a six-well plate filled with 102 m*M* $CaCl_2$. The beads formed within 10 min in the $CaCl_2$ solution (total 4×10^4 cells in 2 mL of gel). After removing the $CaCl_2$ solution from the beads and washing the beads with 155 m*M* NaCl, the medium containing DMEM/F-12 with or without 10% FBS was gently poured on the beads at a volume of 2 mL in a 37°C/5% CO_2 incubator. Throughout the experiment, the medium was changed three times per week. To release the cells, the gel was incubated in 55 m*M* Na citrate at 37°C for 30 min.

In the PuraMatrix™–based 3D culture, 1% of PuraMatrix™ (1 mL) was diluted with chondrocytes (Passage 2) resuspended in 20% sucrose (1 mL). Two milliliter of the mixture containing 4×10^4 cells (density: 2×10^4 cells/mL) was gently poured into the medium containing DMEM/F-12 with or without 10% FBS at a volume of 2 mL in a 37°C/5% CO_2 incubator. The PuraMatrix™ formed 2 mL of gel with a total of 4×10^4 cells within 1 h at 37°C. To release the cells, the gel and cell mixture were aspirated up and down. Throughout the experiment, the medium was changed three times per week. The resuspension was centrifuged at 1000*g* for 5 min to remove the media and the PuraMatrix™.

To evaluate the cell proliferation by cell count, the chondrocytes from three patients were individually incubated in three wells of a six-well plate within each hydrogel material. After a 2-week incubation, the cell numbers were counted by a hematocytometer, while the viability of cells was checked by trypan blue staining.

Chondrocyte culture at high cell density in each hydrogel

Dedifferentiated chondrocytes (Passage 4) were suspended in 0.5% of atelopeptide collagen solution, alginate solution, and PuraMatrix™ solution, at a density of 10^7 cells/mL. In the atelopeptide collagen, 20 μL of the cell/material suspension (total 2×10^5 cells) was placed into the bottom of a 15 mL conical tube to form a gel on 1 h incubation at 37°C. In the case of alginate, 20 μL of the cell/material suspension was dropped into a 15 mL tube filled with 102 m*M* $CaCl_2$. The gel formed within 10 min. The cell/material suspension of PuraMatrix™ (20 μL) was gently poured into the bottom of a 15 mL tube filled with the DMEM/F-12 to form a gel within 1 h at 37°C. The DMEM/F-12 medium was used at a volume of 2 mL for each gel and cultured in a 37°C/5% CO_2 incubator. To induce redifferentiation of the chondrocytes, 5 μg/mL insulin and 200 ng/mL BMP-2 were added to the medium, according to the previous report or its modification.[18,19] As a control without any hydrogel, a cell/medium suspension containing 2×10^5 chondrocytes was centrifuged at 500*g* in a 15 mL conical tube. The supernatant was removed and the resultant pellet was cultured in the DMEM/F-12 without any factors. Throughout the experiment, the medium was changed three times per week.